HHS Public Access

Author manuscript

Mol Cell. Author manuscript; available in PMC 2019 January 08.

Published in final edited form as:

Mol Cell. 2018 June 21; 70(6): 1054–1066.e4. doi:10.1016/j.molcel.2018.05.020.

Spt6 Association with RNA Polymerase II Directs mRNA Turnover During Transcription

Raghuvar Dronamraju[1,2], **Austin J. Hepperla**[3], **Yoichiro Shibata**[2,3], **Alexander T. Adams**[1], **Terry Magnuson**[2,3,4], **Ian J. Davis**[2,3,4,5], and **Brian D. Strahl**[1,2,3,6,*]

[1]Department of Biochemistry & Biophysics, University of North Carolina School of Medicine, Chapel Hill, NC 27599, USA

[2]Lineberger Comprehensive Cancer Center, University of North Carolina School of Medicine, Chapel Hill, NC 27599, USA

[3]Curriculum in Genetics and Molecular Biology, University of North Carolina at Chapel Hill, Chapel Hill, NC 27599, USA

[4]Department of Genetics, The Carolina Center for Genome Sciences, University of North Carolina, Chapel Hill, North Carolina 27599, USA

[5]Departments of Pediatrics, University of North Carolina at Chapel Hill, Chapel Hill, NC 27599, USA

[6]Lead Contact

SUMMARY

Spt6 is an essential histone chaperone that mediates nucleosome reassembly during gene transcription. Spt6 also associates with RNA polymerase II (RNAPII) via a tandem Src2 homology domain. However, the significance of Spt6-RNAPII interaction is not well understood. Here, we show that Spt6 recruitment to genes and its nucleosome reassembly functions are largely independent of association with RNAPII. Instead, the Spt6-RNAPII association mediates recruitment of the Ccr4-Not de-adenylation complex to transcribed genes for essential degradation of a range of mRNAs, including mRNAs required for cell cycle progression. These findings reveal an unexpected control mechanism for mRNA turnover during transcription facilitated by a histone chaperone.

*Correspondence: brian_strahl@med.unc.edu.

AUTHOR CONTRIBUTIONS

R.D. and B.D.S conceived the ideas, designed the experiments, R.D. performed all the experiments with assistance from A.T.A and Y.S. RNA-seq data was analyzed by A.J.H. with input from I.J.D. ATAC-seq libraries were prepared and data were analyzed by Y.S. R.D. and B.D.S. wrote the manuscript with input from all authors.

DECLARATION OF INTERESTS

The authors declare no conflict of interest.

DATA AND SOFTWARE AVAILABILITY

The accession number for the raw and processed RNA-seq and ATAC-seq data reported in this paper is GEO: GSE111815. The raw data reported in this paper has been deposited into Mendeley: http://dx.doi.org/10.17632/tnx4py69j8

INTRODUCTION

Spt6 is an essential replication-independent histone chaperone that was discovered by its ability to alter RNA Polymerase II (RNAPII) transcription start-site selection (Clark-Adams and Winston, 1987; Neigeborn et al., 1987; Swanson et al., 1990). Spt6, which binds H3/H4 dimers and/or tetramers (Bortvin and Winston, 1996; Kaplan et al., 2005; Kaplan et al., 2000), associates with elongating RNAPII and reassembles nucleosomes in the wake of transcription (Diebold et al., 2010; Hartzog et al., 1998; Sdano et al., 2017; Sun et al., 2010). In addition to Spt6, nucleosome reassembly also requires the H2A/H2B-binding FACT (facilitates chromatin transcription) complex, which like Spt6, functions co-transcriptionally (McCullough et al., 2015). As Spt6 maintains chromatin structure in the transcribed region of genes, a hallmark of Spt6 absence or inactivation is inappropriate (cryptic) transcription initiation from within gene bodies (Cheung et al., 2008; DeGennaro et al., 2013; Hainer et al., 2011; Ivanovska et al., 2011; Kaplan et al., 2005; Kaplan et al., 2003). Cryptic transcription, caused by the inactivation of Spt6, was first documented in *Saccharomyces cerevisiae,* but also occurs in the distantly related yeast *Schizosaccharomyces pombe* (Kaplan et al., 2003; Kato et al., 2013a; Kiely et al., 2011). Intriguingly, cryptic transcription in the absence of Spt6 may be bi-directional, producing antisense transcripts that interfere with sense transcription (DeGennaro et al., 2013; Kato et al., 2013a; Kato et al., 2013b). These studies have revealed many facets of Spt6 activity; however, we do not know the complete set of Spt6 functions that contributes to transcriptional regulation.

Spt6 has a key function in transcription elongation by interacting with the phosphorylated serine 2 and tyrosine 1 repeats within the C-terminal domain (CTD) of RNAPII, and with a phosphorylated linker region preceding the CTD (Ardehali et al., 2009; Kwak and Lis, 2013; Mayer et al., 2012; Sdano et al., 2017; Sun et al., 2010). In yeast, Spt6 interaction with phosphorylated tyrosine 1 of RNAPII CTD prevents pre-mature recruitment of termination factors to genes (Mayer et al., 2012). The highly acidic N-terminus of Spt6 interacts with histones and with Spn1/IWS1, another conserved and stable Spt6 binding partner (Mayer et al., 2010; McDonald et al., 2010; Zhang et al., 2008). Although RNAPII interaction provides an attractive explanation for recruitment functions of Spt6 during transcription, significance of this interaction for its functions are less well understood. Likewise, we do not know the precise mechanism by which the Spt6 N-terminus coordinates histone deposition with RNAPII elongation.

In this study, we used a mutant of Spt6 ($spt6_{tSH2\Delta}$) that cannot interact with RNAPII to demonstrate that Spt6-RNAPII interaction is not essential for recruitment of Spt6 to chromatin or for nucleosome deposition. Instead, we found that Spt6-RNAPII interaction is important for full recruitment of Spt6 and RNAPII across genes and for proper mRNA turnover; the latter activity results, in part, from Spt6's recruitment of the Ccr4-Not complex to genes. Consistent with this finding, absence of Spt6-RNAPII interaction caused increased stability of many mRNAs that correlated with an increase of poly(A) tail lengths for a number of transcripts analyzed. Surprisingly, cell cycle-associated transcripts were among the most highly stabilized mRNAs in the absence of Spt6-RNAPII interaction, and, as cell cycle mRNAs must be degraded for cells to progress through the cell cycle, the $spt6_{tSH2\Delta}$ mutant showed cell cycle progression defects. In sum, our findings reveal a critical mRNA

stability control mechanism operating during transcription and an unexpected function for the Spt6 histone chaperone in this mechanism.

RESULTS

Uncoupling Spt6 from RNAPII Reveals Distinct Functions of the Spt6 Chaperone

Spt6 is a transcription-coupled histone chaperone that contains multiple domains, most of which do not have established functions (Figure 1A). Deletion of the Spt6 Helix-hairpin-Helix domain in mutant *spt6–1004* causes nucleosome reassembly defects, cryptic transcription, and decreased Spt6 protein (Cheung et al., 2008; Kaplan et al., 2005; Kaplan et al., 2003). However, *spt6–1004* still interacts with RNAPII (Figure 1B). To determine which functions of Spt6 require its association with RNAPII, we generated a C-terminal truncation of Spt6 ($spt6_{tSH2\Delta}$) that selectively removes the tSH2 RNAPII interaction domain (Figure 1A and 1B) (Dengl et al., 2009; Diebold et al., 2010; Sun et al., 2010; Yoh et al., 2007). We first asked whether $spt6_{tSH2\Delta}$ possesses a *S*u*p*pressor of *T*y (Spt) phenotype. An Spt$^-$ phenotype monitors the ability of RNAPII to utilize an alternate transcription start site to bypass the insertion of a transposable element in the promoters of certain auxotrophic genes such as *HIS4* (Figure 1C), which is otherwise silent under WT conditions (Clark-Adams and Winston, 1987). As expected, *spt6–1004* cells exhibited an Spt$^-$ phenotype (Figure 1D). Intriguingly, however, $spt6_{tSH2\Delta}$ cells showed only a subtle Spt$^-$ phenotype (Figure 1D), indicating that the association of Spt6 with RNAPII is not the critical determinant in Spt6's ability to disrupt Ty element-mediated silencing.

Because $spt6_{tSH2\Delta}$ cells did not possess a strong Spt- phenotype, we asked whether this mutant might instead harbor a transcription elongation defect. To identify such a defect, we spotted wild-type, *spt6–1004,* and $spt6_{tSH2\Delta}$ cells on plates containing 6-Azauracil (6-AU), a drug that depletes rNTPs and that inhibits growth when transcription elongation is otherwise undermined. Both Spt6 mutants were sensitive to 6-AU (Figure 1D) (Hyle et al., 2003), consistent with a function of Spt6 in transcription elongation.

A hallmark of Spt6 loss-of-function alleles is an inability to reassemble chromatin in the wake of RNAPII transcription, causing intragenic or cryptic transcription (DeGennaro et al., 2013; Kaplan et al., 2003; Kato et al., 2013a; Kato et al., 2013b). To test for cryptic transcription, we performed a quantitative real-time PCR (qRT-PCR) assay that monitored the transcript ratio between the 5'- and 3'-ends of genes (Figure 1F). Consistent with previous studies (Kaplan et al., 2003), *spt6–1004* cells at 37°C showed a robust increase in cryptic transcription from several genes known to be susceptible to aberrant intragenic transcription (*STE11, VPS72,* and *SPB4*) (Figure 1G). Conversely, $spt6_{tSH2\Delta}$ cells did not show significant evidence of cryptic transcripts at either 30°C or 37°C (Figure 1H). These data agree with findings of Dengl et al. (Dengl et al., 2009), and the data demonstrated that Spt6 interaction with RNAPII is not required to suppress cryptic transcription.

Finally, we examined additional phenotypes observed for Spt6 mutants to determine which phenotypes, if any, were dependent on Spt6's association with RNAPII. As shown in Figure 1H and 1I, and in agreement with previous findings, the *spt6–1004* mutant was temperature sensitive but not sensitive to several genotoxic agents, *e.g.*, hydroxyurea (HU) and benomyl.

Conversely, *spt6$_{tSH2\Delta}$* cells were heat-resistant and sensitive to the same genotoxic agents. Thus, uncoupling Spt6 from RNAPII creates phenotypes distinct from those associated with other Spt6 mutants that retain RNAPII binding.

The tSH2 domain of Spt6 Contributes to Spt6 and RNAPII Distribution Along Genes

We next assessed the effects of tSH2 domain deletion on Spt6 and RNAPII distribution across genes. Because the *spt6$_{tSH2\Delta}$* mutant showed weak Spt- and cryptic transcription phenotypes, we surmised that *spt6$_{tSH2\Delta}$* was still recruited to genes and performed at least some of the key transcription functions of Spt6. We used ChIP-qPCR to measure the levels and distribution of Spt6 and RNAPII at constitutively expressed genes (*i.e., PMA1* and *TDH3*) in wild-type and *spt6$_{tSH2\Delta}$* cells. As expected for wild-type cells (see Supplementary Figure 1), Spt6 was recruited to both promoter regions and the open reading frames (ORFs) of actively transcribed genes. Consistent with other studies (Cui et al., 2016; Jeronimo et al., 2015; Kaplan et al., 2005; Kaplan et al., 2003; Kaplan et al., 2000; Mayer et al., 2010), the highest levels of Spt6 occurred in ORFs. In contrast, although *spt6$_{tSH2\Delta}$* was still recruited to the transcribed regions of genes, its levels were significantly lower than the levels in wild-type cells. Similarly, the levels of RNAPII were significantly lower in *spt6$_{tSH2\Delta}$* cells compared with wild-type cells at all the assayed genes (Supplementary Figure 1). These results are similar to a requirement of Spt5 in RNAPII recruitment and elongation functions (Shetty et al., 2017). We performed a similar analysis of the effects of the *spt6–1004* allele on Spt6 and RNAPII distribution. Interestingly, on these same genes, the levels of Spt6 were decreased like the tSH2 domain deletion. In addition, the distributions of RNAPII were decreased on the *PMA1 and TDH3* genes (Supplementary Figure 2). Thus, Spt6-RNAPII association is required for proper levels of the RNAPII complexes across transcribed regions, consistent with its role as a transcription elongation factor (Ardehali et al., 2009; Zobeck et al., 2010).

Spt6-RNAPII Interaction Regulates the Global Transcriptome

Because the absence of Spt6-RNAPII interaction led to decreases in Spt6 and RNAPII occupancy on genes, we next determined whether these decreases caused wide-spread changes in transcription. We performed steady state RNA-seq with wild-type and *spt6$_{tSH2\Delta}$* cells under asynchronously growing conditions. As shown in the Bland-Altman plot in Figure 2A and Supplementary Table 1, 2405 genes were upregulated and 485 genes were downregulated in the *spt6$_{tSH2\Delta}$* strain ($p<0.05$, and fold change > 1.4). We next asked whether there was a correlation between the genes that were up/downregulated and gene length or mRNA abundance. We did not detect an association between gene length and transcript abundance ($p = 0.22$; see Figure 2B). However, we observed a significant correlation ($p= 8.19 \times 10^{-20}$) between transcript abundance and changes in expression. Highly expressed genes were associated with decreases in mRNA levels, whereas weakly expressed genes displayed increased abundances. Intriguingly, transcripts downregulated in the *spt6$_{tSH2\Delta}$* mutant were enriched for genes in non-coding RNA metabolism pathways and rRNA processing (Figure 2C and Supplementary Table 1). Upregulated genes in the *spt6$_{tSH2\Delta}$* mutant were significantly enriched for processes including “regulation of RNA metabolism”, which includes genes involved in RNA synthesis and degradation, and “Nuclear Division”, which includes cell cycle-related genes. A further examination of the

genes in the Nuclear Division class verified upregulation of many cell cycle regulators, including B-type Cyclins, *DBF2, CDC28, SWE1,* members of the anaphase promoting complex, and members of the condensin complex (Figure 2D). These results correlate with the observation that $spt6_{tSH2\Delta}$ cells displayed a slow growth phenotype and an elongated bud morphology reminiscent of defects in Cdc28 activation during cell cycle progression (see Figure 3C and (Rudner et al., 2000).

Spt6-RNAPII Interaction is Required for Proper Cell Cycle Progression

Because of the large number of cell cycle-associated genes upregulated in the $spt6_{tSH2\Delta}$ mutant, we tested for a link between Spt6 and cell cycle regulation. Figure 3A depicts the RNA-seq tracks for two representative cell cycle regulators (*CLN2* and *CLB5*) that were upregulated in the $spt6_{tSH2\Delta}$ mutant. *CLN2* is critical for G1/S transition, whereas *CLB5* is critical for S and G2/M phases (Bahler, 2005). An example of a gene unaffected by the $spt6_{tSH2\Delta}$ mutant (linker histone *HHO1*) is also shown in Figure 3A. We next validated these findings by qRT-PCR, which confirmed the observation that cell cycle genes are selectively upregulated in the absence of Spt6-RNAPII interaction (Figure 3B).

Because RNA-seq analysis was performed with asynchronous cultures, we next examined the effect of Spt6-RNAPII uncoupling specifically on transcription of cell cycle genes across the cell cycle. We arrested wild-type and $spt6_{tSH2\Delta}$ mutant cells in G1 with α-factor; following release into fresh medium, cells were collected at several time points across cell cycle. In wild-type cells, qRT-PCR analysis of *CLN2, CLB5,* and *CLB2* (Figure 3D–3F) demonstrated a periodicity that reflected appropriate cell cycle regulation. Conversely, similar regulation was largely absent in the $spt6_{tSH2\Delta}$ mutant. In the $spt6_{tSH2\Delta}$ mutant, all three genes demonstrated a delayed induction and were minimally downregulated. Consistent with the changes in cyclin gene expression across the cell cycle, we found that $spt6_{tSH2\Delta}$ cells had a 15-minute delayed entry into S phase (Figure 3G). Once in S phase, $spt6_{tSH2\Delta}$ cells progressed into the G2/M phase. Significantly, however, $spt6_{tSH2\Delta}$ cells did not exit G2/M at a wild-type rate (Figure 3G). Finally, and consistent with the defects in cell cycle progression and G2/M exit, $spt6_{tSH2\Delta}$ cells exhibited a gross change in morphology (*i.e.*, elongated buds) reminiscent of mutants that compromise Cdc28 activity and mitotic exit (Figure 3C) (Nasmyth, 1993).

To determine whether defects in cell cycle progression in the $spt6_{tSH2\Delta}$ mutant were a direct effect of perturbed Spt6 function instead of a secondary effect of expressing the mutant, we used the anchor away (AA) technique to acutely deplete Spt6 from the nucleus (Haruki et al., 2008). By ChIP-qPCR, we observed that Spt6 levels on *PMA1 and TDH3* chromatin were reduced to about 1.2% of the total levels after 90 minutes of Spt6 nuclear eviction (by rapamycin; Supplementary Figure 3A). We then arrested these cells with α-factor followed by the addition of rapamycin or vehicle control (DMSO) for an additional 90 minutes before cell cycle release (see schematic in Supplementary Figure 3B). After rapamycin treatment or vehicle control, cells were washed and subjected to flow cytometry. The DMSO-treated cells released from G1 arrest followed a normal cell cycle, entering G2/M phase by the expected 60 minutes (Supplementary Figure 3C). In contrast, Spt6 nuclear removal caused a delayed release from G1 arrest (Supplementary Figure 3C). Consistent with our previous qRT-PCR

results showing an increased transcript abundance using the *spt6*$_{tSH2\Delta}$ mutant, we found that cyclin gene expression levels were significantly increased at the 90-minute time points (Supplementary Figure 3D). These data demonstrate that Spt6 association with RNAPII is critical for cell cycle control and regulation of mRNA level.

Spt6-RNAPII interaction is not required for the nucleosome deposition function of Spt6

In light of Spt6's function in nucleosome reassembly, particularly at gene promoters (Perales et al., 2013), we speculated that the upregulation of many genes, including cell cycle-associated genes, in the *spt6*$_{tSH2\Delta}$ mutant may result from improper nucleosome deposition at promoters (an effect that may not be evident from our analyses of cryptic transcription). Control of nucleosome occupancy regulates cell cycle genes (Deniz et al., 2016; Flores et al., 2014; Hogan et al., 2006). To assess whether Spt6-RNAPII interaction might be critical for nucleosome deposition at cell cycle-associated genes, we performed Assay of Transposase-Accessible Chromatin (ATAC-seq) in asynchronously growing wild-type and *spt6*$_{tSH2\Delta}$ cultures (Schep et al., 2015). Contrary to expectation, compared with wild-type cells, we did not observe changes in chromatin accessibility at the promoters of genes upregulated/downregulated in the *spt6*$_{tSH2\Delta}$ mutant (Figure 4A). Specific examination of the ATAC-seq signals at all periodic genes (Spellman et al., 1998) also did not reveal changes in nucleosome occupancy. To confirm these ATAC-seq results, we performed ChIP-qPCR for histones at cell cycle-regulated genes that were upregulated in both asynchronous and synchronized cultures (*i.e., CLN2, CLB5,* and *CLB2*). In the *spt6*$_{tSH2\Delta}$ strain, there were no significant alterations in the H3 and H2B levels in the promoters of these genes (Figure 4B-E). However, histone occupancy was slightly increased in the ORFs of all genes tested; this result was consistent with the finding that nucleosome occupancy is anti-correlated with RNAPII levels on genes (Gilchrist et al., 2010; Schwabish and Struhl, 2004), which we observed in the *spt6*$_{tSH2\Delta}$ mutant (Supplementary Figure 1). Our results indicate that alterations in RNA abundance in the *spt6*$_{tSH2\Delta}$ strain did not result from changes in nucleosome occupancy.

Spt6 is Required for Proper mRNA Turnover

mRNA abundance is a balance between rates of synthesis and degradation (Wilusz et al., 2001). Because the absence of Spt6-RNAPII interaction did not significantly affect nucleosome deposition at promoters, we analyzed nascent (chromatin-bound and un-spliced) and total RNA (processed and mature mRNA) fractions from wild-type and *spt6*$_{tSH2\Delta}$ cells to determine whether there were changes in mRNA synthesis. We assessed the purity of the nascent RNA fraction by estimating the relative enrichment of intron containing RNAs in the nascent and total fractions (Supplementary Figure 4A) (Oesterreich et al., 2016). We subjected the nascent and total RNA fractions to qRT-PCR to measure the relative abundances of cell cycle-regulated transcripts, including *HTA1, CLN2, CLB5,* and *CLB2.* Surprisingly, increased cyclin and histone mRNAs in the *spt6*$_{tSH2\Delta}$ strain was found only in the total fraction (Figure 5A); these same mRNAs were decreased in the nascent (*i.e.*, newly synthesized) fraction (Figure 5B). These results implied that the absence of Spt6-RNAPII interaction caused a decrease in the rate of mRNA synthesis, but, once synthesized, the mRNAs became relatively more stable. The reduced polymerase detected at these genes was consistent with the finding of decreased mRNA synthesis (Supplementary Figure 1).

Because mRNA decay is required for proper gene regulation and cell cycle progression (Das et al., 2017; Haimovich et al., 2013; Medina et al., 2014; Trcek et al., 2011), we next asked whether Spt6-RNAPII interaction regulates mRNA turnover. To measure turnover, we employed the rapid-acting RNA polymerase inhibitor Thiolutin, which enables monitoring of mRNA decay (Coller, 2008; Passos and Parker, 2008). Wild-type and $spt6_{tSH2\Delta}$ cells were grown for 3h followed by addition of Thiolutin. Total cellular RNA was isolated at multiple time points and subjected to qRT-PCR for *CLN2, CLB5*, *CLB2,* and *HTA1.* Strikingly, in the $spt6_{tSH2\Delta}$ strain, all of these genes exhibited increased transcript levels, and all of the transcripts had significantly increased half-lives ($t_{1/2}$) (Figure 5D–5G). These results strongly suggested that the Spt6-RNAPII interaction has a critical function in regulation of mRNA turnover.

To independently verify that the effects on mRNA decay in the $spt6_{tSH2\Delta}$ strain were attributable directly to Spt6 instead of to an indirect effect, we again employed the AA technique (see experimental scheme in Supplementary Figure 5A). We treated cells for 90 minutes with rapamycin or vehicle control followed by the addition of Thiolutin. Samples were collected at indicated time points, and *CLN2, CLB5,* and *CLB2* transcripts were measured by qRT-PCR. The transcript levels of these mRNAs were significantly stabilized with acute nuclear eviction of Spt6 (Supplementary Figure 5B). These results strongly suggest that Spt6 directly regulates mRNA turnover.

Spt6-RNAPII Interaction is Required for Recruitment of the Ccr4-Not Complex to Genes

Because Spt6-RNAPII interaction regulates mRNA turnover, we asked whether the absence of this interaction affects the factors that control mRNA decay. We focused on the Ccr4-Not complex because it functions in various aspects of mRNA metabolism and transcription elongation (Collart and Panasenko, 2012; Dutta et al., 2015; Kerr et al., 2011; Kruk et al., 2011; Miller and Reese, 2012; Reese, 2013; Villanyi and Collart, 2015). Strikingly, the levels of Ccr4, Not1, and Not2 proteins were significantly reduced, albeit to varying degrees, in the $spt6_{tSH2\Delta}$ mutant (Figure 6A). Because the mRNA levels for all of the Ccr4-Not members were not affected (Supplementary Figure 6 and Supplementary Table 1), these data imply that Spt6-RNAPII interaction is required for the stability of the Ccr4-Not complex (Figure 6A).

Because the Ccr4-Not complex interacts with RNAPII (Dutta et al., 2015; Kruk et al., 2011), we next asked whether Ccr4-Not and Spt6 interact via their association with the RNAPII complex. Not1, 2 and 4 levels were extremely low in the $spt6_{tSH2\Delta}$ strain, which excluded them from co-IP studies. Thus, we focused on Ccr4 (Figure 6A). Immunoprecipitation of Spt6 followed by immunoblot analysis for Ccr4 demonstrated an interaction between Ccr4 and Spt6 (Figure 6B). Significantly, deletion of the Spt6-tSH2 domain did not completely disrupt this interaction, albeit there were reduced the levels of co-immunoprecipitated Ccr4-Myc given the input levels were also lower. These results suggest that the association of Spt6 with Ccr4 is not mediated by co-association with RNAPII and point to a more direct interaction between Spt6 and the Ccr4-Not complex.

Because the input levels of Ccr4-Not complex members were affected in the $spt6_{tSH2\Delta}$ strain, we again employed the AA technique to examine the stability and recruitment of

Ccr4-Not members to genes upon acute nuclear depletion of Spt6. Treatment of cells with rapamycin for 30 or 90 minutes to deplete Spt6 from the nucleus did not affect the protein levels of Ccr4 and Not2 (Figure 6C). However, prolonged rapamycin treatment (>3h) resulted in a decrease of Ccr4 similar to that observed in the *spt6*$_{tSH2\Delta}$ strain (Figure 6D). Because Ccr4-Not levels remained intact at early time points of Spt6 nuclear eviction, we performed ChIP-qPCR to measure the effect of Spt6 nuclear removal on Spt6, Ccr4, and Not2 occupancy at the *PMA1* and *TDH3* loci (Figure 6E and 6F). Within 30 minutes of rapamycin treatment, ~85% of Spt6 was depleted from *PMA1* and *TDH3* (Figure 6G and 6H). Strikingly, chromatin levels of Ccr4 (Figure 6I, 6J) and Not2 (Figure 6K, and 6L) were depleted with kinetics similar to that of Spt6. In contrast, RNAPII depletion from these same genes (Figure 6M, and 6N) occurred with slower kinetics and was detectable on these genes at the 30 min timepoint (a 11.3-fold reduction in the levels of Spt6 compared to 3-fold reduction in RNAPII at the 30 minute timepoint). These results provide further support for the idea that Spt6 directly recruits the Ccr4-Not complex to genes.

Spt6-RNAPII Interaction Regulates mRNA Deadenylation and Decay

In view of the unexpected connection between Spt6 and the Ccr4-Not complex, we asked whether disrupting Spt6-RNAPII interaction would result in RNA processing defects similar to defects observed in Ccr4 mutants (*i.e.*, decreased deadenylation and slower mRNA decay). Thus, we performed high resolution Northern Blot analyses of the *spt6*$_{tSH2\Delta}$ strain and a *CCR4* deletion strain (*ccr4Δ*) to examine the poly(A) tail lengths of transcripts regulated by Spt6-RNAPII interaction (*HTA1* and *CLB5*). For a control, we analyzed the mRNA levels of *RPL46A*, a transcript not found to be regulated by Spt6-RNAPII interaction. Poly(A) tail length was resolved by digesting total RNA with RNAse H in the presence of a gene specific 3'-end primer and oligo-dT to generate a completely deadenylated transcript (A_0) or a gene specific primer to measure only the poly(A) tail length (Hu and Coller, 2013; Tucker et al., 2002; Tucker et al., 2001). We found that poly(A) tail lengths for *HTA1* and *CLB5* were increased in both the *spt6*$_{tSH2\Delta}$ and *ccr4Δ* mutant strains compared with wild-type (Figure 6O). Conversely, no increases in poly(A) tail length in the *RPL46A* transcript were observed in any mutant strain (Figure 6M).

To ascertain whether the *spt6*$_{tSH2\Delta}$ mutant also affected deadenylation kinetics, we employed the *GAL* gene model of transcriptional shut-off previously used to make kinetic assessments of mRNA turnover rates with mutants of the Ccr4-Not complex (Tucker et al., 2002; Tucker et al., 2001). As expected in wild-type cells, *GAL10* mRNA was maximally induced within 15 minutes of galactose addition and was repressed (with its mRNA fully degraded) within 10 minutes following dextrose addition (Figure 6P). In stark contrast, induction of *GAL10* was dramatically impaired in the *spt6*$_{tSH2\Delta}$ strain, and, further, its rate of mRNA decay was also significantly delayed compared with wild-type (~10 minutes) (Figure 6N). These results reinforce the finding that Spt6 controls mRNA decay processes partly by deadenylation, in addition to the important function of Spt6-RNAPII interaction in transcriptional regulation.

DISCUSSION

Although Spt6 has been well studied during transcription elongation, the full range of Spt6's contributions to transcription have not been fully elucidated. In this study, we show that Spt6-RNAPII interaction is vital to the maintenance of mRNA turnover during transcription, a requirement that is likely explained by the fact that Spt6 recruits the Ccr4-Not mRNA deadenylation complex to genes (Figure 7). Until now, Spt6 was primarily thought to contribute to transcription by promoting RNAPII elongation and/or by reassembling nucleosomes in the wake of RNAPII transcription. Our data expand the repertoire of Spt6 transcriptional activities to include a function in mRNA homeostasis.

Although the function of the N-terminus of Spt6 in regulating histone/nucleosome reassembly has received much attention, the function of its C-terminus, which mediates RNAPII interaction via its tSH2 domain (Chiang et al., 1996; Close et al., 2011; Dengl et al., 2009; Diebold et al., 2010; Yoh et al., 2007), is less clear. We expected that Spt6-RNAPII interaction would be important for Spt6 recruitment to genes and nucleosome reassembly during transcription. However, our studies point to a completely unexpected Spt6 activity in that Spt6-RNAPII uncoupling caused defects in the global transcriptome without nucleosome reassembly change. Our studies explain how Spt6-RNAPII uncoupling causes significant upregulation of many weakly transcribed genes (i.e., increased mRNA stability); however, they do not explain why highly transcribed genes require Spt6-RNAPII interaction for optimal expression (Figure 2A). Perhaps highly transcribed genes are either less reliant on the Ccr4-Not pathway for their regulation or they are more dependent on the elongation-stimulating activity of Spt6.

Our finding that Spt6 associates with the Ccr4-Not complex provides a mechanistic basis for Spt6 control of mRNA turnover. The association between Spt6 and Ccr4-Not also likely explains how Spt6 recruits Ccr4-Not genes. However, more work is needed to determine whether Ccr4-Not interaction occurs directly with Spt6 or indirectly with other Spt6-associated factors (*e.g.*, Spt4/Spt5). In addition, our Spt6/Ccr4-Not interaction findings contrast with those of Denis et al. who did not detect Spt6 in Ccr4 immunoprecipitates (Denis et al., 1994). The absence of Spt6-Ccr4 co-immunoprecipitation in the earlier study may have been due to the transient, and perhaps indirect, nature of the Spt6-Ccr4 interaction (Denis et al., 1994).

In addition to showing that Spt6 associates with Ccr4-Not, we found that Spt6-RNAPII uncoupling and long-term nuclear depletion of Spt6 impaired the stability of members of the Ccr4-Not complex. Although we do not know the mechanism of this accelerated protein turnover, these results suggest that recruitment of the Ccr4-Not complex to chromatin is critical for the stability and function of the complex. Intriguingly, Ccr4-Not is nuclear, where it functions in transcription elongation, and cytoplasmic, where it is involved in deadenylation (Collart, 2016; Siwaszek et al., 2014). Thus, our findings suggest that chromatin association is an important event in the life-cycle and long-term cytoplasmic function and stability of the Ccr4-Not complex. But how would this occur and why would this regulation be necessary? We speculate that loading of Ccr4-Not onto genes undergoing transcription may facilitate subsequent mRNA binding (via its numerous RNA interaction

motifs) (Collart and Reese, 2014; Villanyi and Collart, 2015) to nascent RNA, which may serve to maintain this complex's stability and export into the cytoplasm. We further speculate that the association of Ccr4-Not with mRNA from initial transcription to translation may facilitate rapid and timely degradation of mRNAs expressed in rapidly changing transcription programs such as the cell cycle (Eser et al., 2014). Indeed, mutations in other genes (*e.g.*, Xrn1, Dbf2, and Dhh1) that impair mRNA degradation also show morphological and cell cycle phenotypes similar to $spt6_{tSH2\Delta}$ cells (Maillet et al., 2000; Manukyan et al., 2008; Traven et al., 2009; Westmoreland et al., 2004). Further, our studies showed that deletion of *CCR4* leads to sensitivity to genotoxic agents and a delay in release from G1 arrest, phenotypes that are also possessed by $spt6_{tSH2\Delta}$ cells (Supplementary Figure 7).

Although we have discovered a function for Spt6-dependent gene recruitment of Ccr4-Not in the regulation of mRNA stability, it is possible that the stabilization of a significant fraction of mRNAs may also be an effect of a global decrease in transcription (Dahan and Choder, 2013; Goler-Baron et al., 2008; Haimovich et al., 2013; Shalem et al., 2011). Several studies have demonstrated the existence of a feedback loop between mRNA synthesis and decay leading to maintenance of global mRNA levels (*i.e.*, "buffering") (Sun et al., 2013; Sun et al., 2012). Our analysis of several transcripts (Figure 5B) whose steady state levels increased were, in fact, down-regulated when examining the nascent levels of those RNAs. Thus, a feedback mechanism between the rates of mRNA synthesis and degradation may also contribute to the stability of these mRNAs in addition to our reported connection between Spt6 and the Ccr4-Not complex. Finally, promoter elements are also suggested to control the fate of mRNAs, such that genes that share promoter elements are transcribed and degraded in a similar manner, providing an additional layer of tight control of gene expression (Bregman et al., 2011; Enssle et al., 1993; Trcek et al., 2011). There is no information pointing to a function of Spt6 in recognizing specific promoter elements, which precludes promoters from the regulation of mRNA stability in the $spt6_{tSH2\Delta}$ cells in this study.

In conclusion, our studies reveal an important function for Spt6-RNAPII interaction in regulation of the global transcriptome and in mRNA turnover, which is key for proper cell cycle progression. Because of the high evolutionarily conservation of Spt6, we predict that these findings will be mirrored in more complex eukaryotes and critical to the regulation of transcription programs that govern animal development, cell fate specification, and disease progression.

STAR METHODS

CONTACT FOR REAGENT AND RESOURCE SHARING

Further information and requests for resources and reagents should be directed to, and will be fulfilled by, the Lead Contact, Brian D. Strahl (brian_stral@med.unc.edu).

EXPERIMENTAL MODEL AND SUBJECT DETAILS

All yeast strains, plasmids, antibodies, and general reagents used in this study are listed in Supplementary Table 2. Deletion and C-terminal tagging were performed using the PCR tool box as described (Gelbart et al., 2001; Janke et al., 2004). All yeast strains used in this study were verified by PCR, Sanger sequencing, and immunoblotting for the respective epitopes.

METHOD DETAILS

SPT6 ANCHOR AWAY—A strain containing an FRB-tagged form of Spt6 was treated with 1 μg/ml of rapamycin to deplete Spt6 from the nucleus (Fan et al., 2011). Cells were collected at indicated time points and fixed in formaldehyde immediately for ChIP assays. The percent Spt6 remaining in the nucleus at indicated time points was calculated using ChIP-qPCR at the *PMA1* and *TDH3* loci.

SPOTTING ASSAYS—Saturated yeast cultures of the indicated genotypes were diluted five-fold and spotted on plates with or without 200 mM hydroxyurea (HU), 200 μg/ml of 6-azauracil (6-AU), or 20 μg/ml of benomyl. To assess a *SPT*$^-$ phenotype, cells were spotted on either SC or SC-LYS and allowed to grow for 3 days before taking photographs. Strains used for 6-AU assays contained a pRS316 *URA3*-containing plasmid. Growth was assessed after 3 days at 30°C or 37°C as indicated. All experiments were performed at least three times.

CO-IMMUNOPRECIPITATION OF PROTEIN COMPLEXES—Co-immunoprecipitation was performed using an established method (Moqtaderi et al., 1996). Briefly, an overnight saturated yeast culture was diluted in 100 ml of YPD to an OD_{600} of 0.2 and grown subsequently for 4 h to an OD_{600} of ~1.0. Cells were washed once with ice cold water and lysed in 600 μl lysis buffer [450 mM Tris-acetate (pH 7.8), 150 mM potassium acetate, 60% (v/v) glycerol, 3 mM EDTA (pH 8.0), supplemented with fresh 1 mM DTT, 1 mM PMSF, 1X complete EDTA-free protease inhibitors (Roche)] using standard bead-beating procedures as described. Lysates were then clarified by centrifugation for 15 minutes 4°C. One mg of total protein (estimated using Bradford) was incubated with the indicated antibody overnight at 4°C in 1 ml of buffer A [50 mM HEPES-KOH (pH 7.5), 1 mM EDTA (pH 8.0), 20% (v/v) glycerol, 125 mM potassium acetate, 1% (v/v) NP-40, supplemented with fresh 100 mM DTT]. Protein A Agarose beads (Sigma Aldrich) were added and incubated for 2 h at 4°C. The complexes on beads were washed 3 times in buffer A. Beads were heated at 95°C and proteins were separated by SDS-PAGE and subjected to immunoblotting to detect interacting proteins.

IMMUNOBLOTTING—Immunoblotting was performed after extraction of proteins by TCA lysis as described (Keogh et al., 2006a; Keogh et al., 2006b). Lysates were separated by SDS-PAGE and probed using primary antibodies described in Supplementary Table 2. HRP-conjugated anti-rabbit (GE Healthcare, NA934V; 1:10,000) or anti-mouse secondary (GE Healthcare, NA931V; 1:10,000) antibodies were used for detection by ECL Prime or enhanced chemiluminescence ECL (Amersham Biosciences).

RNA-SEQ AND QRT-PCR METHODOLOGY—WT and *spt6*$_{tSH2\Delta}$ strains were cultured in YPD for 4 h after diluting overnight saturated cultures to an OD_{600} of 0.2. RNA was extracted from the cells using an acid-phenol method as described. Residual DNA was eliminated by DNase treatment (DNAse I, Ambion Cat #AM2222). Library preparation and sequencing were performed at the High-Throughput Sequencing Facility (HTSF) at UNC Chapel Hill. Libraries were prepared using TruSeq Stranded Total RNA with RiboZero Gold Library Prep Kit (Illumina) and were sequenced using Illumina HiSeq 2500 (50 bp, single-end reads). One microgram of total RNA was used to generate cDNA from Random hexamer primers and Superscript Reverse Transcriptase III (Thermo-Fisher Scientific, 108–80044). The cDNA was diluted 1:25 before measuring the relative abundance of the transcripts. The real-time PCR primers employed will be provided upon request. Quantitative real-time PCR was performed using SYBR Green Master mix (Bio-Rad, 1725270), and the relative abundances of the transcripts were calculated using the Livak method (Livak et al., 2013). *SCR1* served as a normalization control. Data shown are the replicates of three independent experiments; the significance values were calculated using Student t-test.

RNA-SEQ READ ALIGNMENTS AND ANALYSIS—RNA-seq libraries were sequenced on the Illumina HiSeq 2500. Reads containing Illumina adapter sequences were filtered out via TagDust (v1.12) with an FDR cutoff of 0.001. Reads were then aligned to the sacCer3 genome using Bowtie (v1.1.2) with options -m 1, --seed=123, and --nomaqround. Post-alignment, Samtools (v0.1.9) and bedtools (v2.25.0) were used to interconvert files. Gene counts were calculated using HTSeq (v0.6.1) and the sacCer3 sgdGene table from UCSC Genome Browser, and DESeq2 (v1.6.3) in R (v3.1.1) was used to identify differentially abundant mRNA. Gene expression in reads per kilobase per million mapped reads (RPKM) was calculated using in-house scripts. Only genes that had both a DESeq2 adjusted p-value < 0.05 and a $\log_2$(RPKM fold change) of at least 0.5 in either direction were considered for downstream analyses. GO terms were generated using DAVID (v6.8). The accession numbers for the RNA-seq and ATAC-seq datasets reported in this paper are through GEO (accession no. GSE 111815).

CHROMATIN FRACTIONATION AND NASCENT RNA EXTRACTION—Nascent chromatin-bound RNA was extracted form yeast cells as described (Oesterreich et al., 2016). Briefly, 250 ml of wild-type and *spt6*$_{tSH2\Delta}$ strains were grown to an OD_{600} ~1, collected by centrifugation, and washed twice in PBS. Chromatin fractions were prepared as described by Carrillo et al. The chromatin fractions were resuspended in 250 μl of 50 mM NaAcetate pH 5.0, 50 mM NaCl, 1% SDS, and RNA was extracted from the chromatin fraction using an acid phenol method as described. RNA was subjected to DNAse treatment, and the enrichment of nascent transcripts was calculated using gene specific primers designed for *ADH1* as described (Oesterreich et al., 2016). Total and Nascent RNA were subjected to qRT-PCR to detect changes in the levels of different cyclin and histone mRNAs.

mRNA STABILITY MEASUREMENTS—Thiolutin, an inhibitor of all forms of RNA polymerase, was used to measure the mRNA decay rates as described previously (Coller, 2008). Briefly, wild type and *spt6*$_{tSH2\Delta}$ strains were grown to mid log phase in YPD to an

OD_{600} of about 0.6. Thiolutin was added to 5 μg/ml, and cells were collected at indicated time points and flash frozen in liquid nitrogen. RNA was extracted and the relative abundance at each time point was measured by qRT-PCR as described above. To assess a direct role of Spt6 in the regulation of mRNA stability, we depleted Spt6 from the nucleus using 1 μg/ml rapamycin for 90 minutes, after which the cells were treated immediately with 5 μg/ml of Thiolutin. Cells were collected at indicated time intervals and used for RNA extraction and qRT-PCR measurements.

ANALYSIS OF mRNA DECAY RATES—RNA was extracted using acid phenol method as described previously. Poly(A) tail length and rates of mRNA decay were measured by Northern Blotting of RNAs cleaved at the 3' ends using a gene specific primer only or a combination of gene specific primer and oligo-dT to measure the totally de-adenylated RNA as described (Muhlrad et al., 1994). Briefly, gene specific primer (GSP) and/or oligo-$dT_{12–18}$ primers of candidate genes were hybridized to total RNA at 68°C for 10 minutes in hybridization buffer (250mM Tris-HCl pH7.5, 1mM EDTA and 50mM NaCl). The reaction was allowed to cool and the mixture was treated with 1U of RNAse H for 60 minutes at 37°C. The reaction was stopped using stop mix (0.04 mg/ml tRNA, 20 mM EDTA and 300 mM sodium acetate). RNA was extracted by phenol chloroform method and resuspended in 10 μL of DEPC-treated water. RNA was mixed with equal volumes of RNA loading buffer and separated in 8% −10% TBE-urea-polyacrylamide gels at constant power (10W). RNA was electroblotted onto ZetaProbe membranes at 250mA for 2h and then at 350mA for a further 2h at 4°C and probed using gamma-^{32}P-labeled oligos, which are available upon request. Dried membranes were exposed to FujiFilm Imaging plate for 24 hrs. The imaging plate was scanned on a Typhoon Trio Variable mode Imager.

ATAC-SEQ LIBRARY PREPARATION—Five million wild-type (S288C) and *spt6*$_{tSH2\Delta}$ cells were collected during their linear phase of growth. Three replicates each were collected for the wild type and mutant (total of 6 replicates). ATAC-seq libraries were made as described (Buenrostro et al., 2015; Schep et al., 2017), with the exception of a double-sided SPRI bead size selection step of each library, using 0.5× and 1× ratio of SPRI beads to obtain a library size range of ~150 bp to ~2 kb. Wild type replicates were index labeled using Ad2.1_TAAGGCGA, Ad2.2_CGTACTAG, and Ad2.3_AGGCAGAA Illumina indexes, whereas the mutant libraries were indexed using Ad2.6_TAGGCATG, Ad2.7_CTCTCTAC, and Ad2.8_CAGAGAGG (Buenrostro 2013). All 6 libraries were combined and sequenced on a single lane of Illumina Hiseq 2500 using v4 chemistry for 50bp paired-end output.

ATAC-SEQ ALIGNMENTS AND INITIAL ANALYSIS—Fastq sequence files were first filtered for high quality reads using trimgalore version 0.4.1, "trim_galore -q 20 --nextera --length 20", then aligned to the sacCer3 genome using bowtie2, "bowtie2 --threads 6 --very-sensitive --maxins 2000" (Krueger 2015 and Langmead 2012). bowtie2 output files were converted to bam files using Samtools version 1.3.1. Next Bedtools version 2.25.0 "bamtobed" was used to convert bam output files to bed file format to perform the subsequent steps (Quinlan 2010). Using simple custom Awk scripts, exact Tn5 transposase bp insertion sites were created from the bed files by adjusting the insertion sites +4 bp for

positive strand sequences, adjusting −5 bp for negative stranded sequences, and adjusting the bed file region to just the 1 bp region at the insertion sites. This bed file was then converted back to bam format using Bedtools “bedtobam” before normalizing the sequence counts using Deeptools’ bamCoverage, “ --binSize 1 --fragmentLength 1 --normalizeTo1× 12100000 --minMappingQuality 20”, to create a bigWig output file for each replicate.

Awk command with For loop:

for i in ./s_*/bowtie2_sacCer3; do

awk ‘BEGIN OFS = “\t”; if ($6 == “+”) print $1, $2 + 4, $2 + 5, $4, $5, $6; else print $1, $3 – 6, $3 – 5, $4, $5, $6}’ $i/sequence.bed > $i/sequence.shifted.exactcut.bed; done

META-ANALYSIS OF ATAC-SEQ SIGNAL—Differential genes determined using DESeq2 were used to create a list of upregulated (567) and downregulated (598) genes in the mutant yeast strain compared with the wild type. A similar number of genes (601) was selected for which the expression levels had little or no change (DESeq2, padj>0.5) but which reflected a range of baseline transcription levels. Cell cycle (800 genes, Spellman 1998) and histone (8 genes) gene lists were compiled. Each set of genes was sorted in decreasing order from highest transcribed to lowest transcribed. Using computematrix.py and plotheatmapper.py programs from Deeptools version 2.2.4, we normalized ATAC-seq signal for a scaled region representing each of the genes in our gene subsets plus/minus 1 kb were compiled and plotted (Borrill et al., 2016).

YEAST CELL CYCLE SYNCHRONIZATION—Saturated cultures of the wild type and $spt6_{tSH2\Delta}$ strains were inoculated into YPD at an OD_{600} of 0.1 and allowed to grow to an OD_{600} ~0.6. Alpha-factor (25 nM; GenScript USA, RPO1002) was added to cultures to arrest cells in the G1-phase of cell cycle. G1 arrest was confirmed by microscopy. G1-arrested cells were washed three time in water and released into fresh YPD medium. Samples were collected at indicated time points for propidium iodide staining to assess the population distribution across different phases of cell cycle, and additional samples were collected in parallel for RNA extraction and cDNA synthesis. FRB-tagged *SPT6* strains were treated with α-factor to induce G1-arrest for 2 h, followed by the addition of 1 μg/ml of rapamycin for 90 minutes. After the treatments, cells were washed and released into fresh YPD medium. At indicated time intervals, cells were collected and flash frozen in liquid nitrogen for RNA extraction and qRT-PCR. Cells were also collected at the same time intervals and fixed in 70% ethanol to measure their cell cycle distribution by flow cytometry of propidium iodide-stained nuclei.

CHROMATIN IMMUNOPRECIPITATION—ChIP was performed as described with modifications (Ahn et al., 2009). DNA was eluted in 100 μl of elution buffer. Two μl of the DNA was subjected to qPCR using SYBR Green (Bio-Rad), and the data were analyzed as described. Data are representative of three independent replicates. Data are represented as the mean percent input values over standard deviations (SD) from three biological replicates with technical triplicates.

Supplementary Material

Refer to Web version on PubMed Central for supplementary material.

ACKNOWLEDGMENTS

We sincerely acknowledge the help provided by Joseph B. Bridgers in expressing and purifying the DLD domain of Spt6 for antisera generation, Josh Boyer and Jared Baisden (Qi Zhang lab) and William Marzluff at UNC for all their support and expert advice on Northern Blotting protocols. We thank the UNC high-throughput sequencing facility and the members of B.D.S. and T.M. labs for their support and Howard Fried for editorial help. B.D.S. acknowledges support from NIH grants R35GM126900 and R01GM110058, and I.J.D. acknowledges support from NIH grants CA166447 and CA198482 and the Corn-Hammond Fund for Pediatric Oncology.

REFERENCES

Ahn SH, Keogh MC, and Buratowski S (2009). Ctk1 promotes dissociation of basal transcription factors from elongating RNA polymerase II. EMBO J 28, 205–212. [PubMed: 19131970]

Ardehali MB, Yao J, Adelman K, Fuda NJ, Petesch SJ, Webb WW, and Lis JT (2009). Spt6 enhances the elongation rate of RNA polymerase II in vivo. EMBO J 28, 1067–1077. [PubMed: 19279664]

Bahler J (2005). Cell-cycle control of gene expression in budding and fission yeast. Annu Rev Genet 39, 69–94. [PubMed: 16285853]

Borrill P, Ramirez-Gonzalez R, and Uauy C (2016). expVIP: a Customizable RNA-seq Data Analysis and Visualization Platform. Plant Physiol 170, 2172–2186. [PubMed: 26869702]

Bortvin A, and Winston F (1996). Evidence that Spt6p controls chromatin structure by a direct interaction with histones. Science 272, 1473–1476. [PubMed: 8633238]

Bregman A, Avraham-Kelbert M, Barkai O, Duek L, Guterman A, and Choder M (2011). Promoter elements regulate cytoplasmic mRNA decay. Cell 147, 1473–1483. [PubMed: 22196725]

Buenrostro JD, Wu B, Litzenburger UM, Ruff D, Gonzales ML, Snyder MP, Chang HY, and Greenleaf WJ (2015). Single-cell chromatin accessibility reveals principles of regulatory variation. Nature 523, 486–490. [PubMed: 26083756]

Cheung V, Chua G, Batada NN, Landry CR, Michnick SW, Hughes TR, and Winston F (2008). Chromatin- and transcription-related factors repress transcription from within coding regions throughout the Saccharomyces cerevisiae genome. PLoS Biol 6, e277. [PubMed: 18998772]

Chiang PW, Wang S, Smithivas P, Song WJ, Ramamoorthy S, Hillman J, Puett S, Van Keuren ML, Crombez E, Kumar A, et al. (1996). Identification and analysis of the human and murine putative chromatin structure regulator SUPT6H and Supt6h. Genomics 34, 328–333. [PubMed: 8786132]

Clark-Adams CD, and Winston F (1987). The SPT6 gene is essential for growth and is required for delta-mediated transcription in Saccharomyces cerevisiae. Mol Cell Biol 7, 679–686. [PubMed: 3029564]

Close D, Johnson SJ, Sdano MA, McDonald SM, Robinson H, Formosa T, and Hill CP (2011). Crystal structures of the S. cerevisiae Spt6 core and C-terminal tandem SH2 domain. J Mol Biol 408, 697–713. [PubMed: 21419780]

Collart MA (2016). The Ccr4-Not complex is a key regulator of eukaryotic gene expression. Wiley Interdiscip Rev RNA 7, 438–454. [PubMed: 26821858]

Collart MA, and Panasenko OO (2012). The Ccr4--not complex. Gene 492, 42–53. [PubMed: 22027279]

Collart MA, and Reese JC (2014). Gene expression as a circular process: cross-talk between transcription and mRNA degradation in eukaryotes; International University of Andalusia (UNIA) Baeza, Spain. RNA Biol 11, 320–323. [PubMed: 24646520]

Coller J (2008). Methods to determine mRNA half-life in Saccharomyces cerevisiae. Methods Enzymol 448, 267–284. [PubMed: 19111181]

Cui P, Jin H, Vutukuru MR, and Kaplan CD (2016). Relationships Between RNA Polymerase II Activity and Spt Elongation Factors to Spt- Phenotype and Growth in Saccharomyces cerevisiae. G3 (Bethesda) 6, 2489–2504. [PubMed: 27261007]

Dahan N, and Choder M (2013). The eukaryotic transcriptional machinery regulates mRNA translation and decay in the cytoplasm. Biochim Biophys Acta 1829, 169–173. [PubMed: 22982191]

Das S, Sarkar D, and Das B (2017). The interplay between transcription and mRNA degradation in Saccharomyces cerevisiae. Microb Cell 4, 212–228. [PubMed: 28706937]

DeGennaro CM, Alver BH, Marguerat S, Stepanova E, Davis CP, Bahler J, Park PJ, and Winston F (2013). Spt6 regulates intragenic and antisense transcription, nucleosome positioning, and histone modifications genome-wide in fission yeast. Mol Cell Biol 33, 4779–4792. [PubMed: 24100010]

Dengl S, Mayer A, Sun M, and Cramer P (2009). Structure and in vivo requirement of the yeast Spt6 SH2 domain. J Mol Biol 389, 211–225. [PubMed: 19371747]

Denis CL, Draper MP, Liu HY, Malvar T, Vallari RC, and Cook WJ (1994). The yeast CCR4 protein is neither regulated by nor associated with the SPT6 and SPT10 proteins and forms a functionally distinct complex from that of the SNF/SWI transcription factors. Genetics 138, 1005–1013. [PubMed: 7896086]

Deniz O, Flores O, Aldea M, Soler-Lopez M, and Orozco M (2016). Nucleosome architecture throughout the cell cycle. Sci Rep 6, 19729. [PubMed: 26818620]

Diebold ML, Loeliger E, Koch M, Winston F, Cavarelli J, and Romier C (2010). Noncanonical tandem SH2 enables interaction of elongation factor Spt6 with RNA polymerase II. J Biol Chem 285, 38389–38398. [PubMed: 20926373]

Dutta A, Babbarwal V, Fu J, Brunke-Reese D, Libert DM, Willis J, and Reese JC (2015). Ccr4-Not and TFIIS Function Cooperatively To Rescue Arrested RNA Polymerase II. Mol Cell Biol 35, 1915–1925. [PubMed: 25776559]

Enssle J, Kugler W, Hentze MW, and Kulozik AE (1993). Determination of mRNA fate by different RNA polymerase II promoters. Proc Natl Acad Sci U S A 90, 10091–10095. [PubMed: 8234261]

Eser P, Demel C, Maier KC, Schwalb B, Pirkl N, Martin DE, Cramer P, and Tresch A (2014). Periodic mRNA synthesis and degradation co-operate during cell cycle gene expression. Mol Syst Biol 10, 717. [PubMed: 24489117]

Fan X, Geisberg JV, Wong KH, and Jin Y (2011). Conditional depletion of nuclear proteins by the Anchor Away system. Curr Protoc Mol Biol *Chapter* 13, Unit13 10B.

Flores O, Deniz O, Soler-Lopez M, and Orozco M (2014). Fuzziness and noise in nucleosomal architecture. Nucleic Acids Res 42, 4934–4946. [PubMed: 24586063]

Gelbart ME, Rechsteiner T, Richmond TJ, and Tsukiyama T (2001). Interactions of Isw2 chromatin remodeling complex with nucleosomal arrays: analyses using recombinant yeast histones and immobilized templates. Mol Cell Biol 21, 2098–2106. [PubMed: 11238944]

Gilchrist DA, Dos Santos G, Fargo DC, Xie B, Gao Y, Li L, and Adelman K (2010). Pausing of RNA polymerase II disrupts DNA-specified nucleosome organization to enable precise gene regulation. Cell 143, 540–551. [PubMed: 21074046]

Goler-Baron V, Selitrennik M, Barkai O, Haimovich G, Lotan R, and Choder M (2008). Transcription in the nucleus and mRNA decay in the cytoplasm are coupled processes. Genes Dev 22, 2022–2027. [PubMed: 18676807]

Haimovich G, Medina DA, Causse SZ, Garber M, Millan-Zambrano G, Barkai O, Chavez S, Perez-Ortin JE, Darzacq X, and Choder M (2013). Gene expression is circular: factors for mRNA degradation also foster mRNA synthesis. Cell 153, 1000–1011. [PubMed: 23706738]

Hainer SJ, Pruneski JA, Mitchell RD, Monteverde RM, and Martens JA (2011). Intergenic transcription causes repression by directing nucleosome assembly. Genes Dev 25, 29–40. [PubMed: 21156811]

Hartzog GA, Wada T, Handa H, and Winston F (1998). Evidence that Spt4, Spt5, and Spt6 control transcription elongation by RNA polymerase II in Saccharomyces cerevisiae. Genes Dev 12, 357–369. [PubMed: 9450930]

Haruki H, Nishikawa J, and Laemmli UK (2008). The anchor-away technique: rapid, conditional establishment of yeast mutant phenotypes. Mol Cell 31, 925–932. [PubMed: 18922474]

Hogan GJ, Lee CK, and Lieb JD (2006). Cell cycle-specified fluctuation of nucleosome occupancy at gene promoters. PLoS Genet 2, e158. [PubMed: 17002501]

Hu W, and Coller J (2013). Method for measuring mRNA decay rate in Saccharomyces cerevisiae. Methods Enzymol 530, 137–155. [PubMed: 24034319]

Hyle JW, Shaw RJ, and Reines D (2003). Functional distinctions between IMP dehydrogenase genes in providing mycophenolate resistance and guanine prototrophy to yeast. J Biol Chem 278, 28470–28478. [PubMed: 12746440]

Ivanovska I, Jacques PE, Rando OJ, Robert F, and Winston F (2011). Control of chromatin structure by spt6: different consequences in coding and regulatory regions. Mol Cell Biol 31, 531–541. [PubMed: 21098123]

Janke C, Magiera MM, Rathfelder N, Taxis C, Reber S, Maekawa H, Moreno-Borchart A, Doenges G, Schwob E, Schiebel E, et al. (2004). A versatile toolbox for PCR-based tagging of yeast genes: new fluorescent proteins, more markers and promoter substitution cassettes. Yeast 21, 947–962. [PubMed: 15334558]

Jeronimo C, Watanabe S, Kaplan CD, Peterson CL, and Robert F (2015). The Histone Chaperones FACT and Spt6 Restrict H2A.Z from Intragenic Locations. Mol Cell 58, 1113–1123. [PubMed: 25959393]

Kaplan CD, Holland MJ, and Winston F (2005). Interaction between transcription elongation factors and mRNA 3'-end formation at the Saccharomyces cerevisiae GAL10-GAL7 locus. J Biol Chem 280, 913–922. [PubMed: 15531585]

Kaplan CD, Laprade L, and Winston F (2003). Transcription elongation factors repress transcription initiation from cryptic sites. Science 301, 1096–1099. [PubMed: 12934008]

Kaplan CD, Morris JR, Wu C, and Winston F (2000). Spt5 and spt6 are associated with active transcription and have characteristics of general elongation factors in D. melanogaster. Genes Dev 14, 2623–2634. [PubMed: 11040216]

Kato H, Okazaki K, Iida T, Nakayama J, Murakami Y, and Urano T (2013a). Spt6 prevents transcription-coupled loss of posttranslationally modified histone H3. Sci Rep 3, 2186. [PubMed: 23851719]

Kato H, Okazaki K, and Urano T (2013b). Spt6: two fundamentally distinct functions in the regulation of histone modification. Epigenetics 8, 1249–1253. [PubMed: 24107707]

Keogh MC, Kim JA, Downey M, Fillingham J, Chowdhury D, Harrison JC, Onishi M, Datta N, Galicia S, Emili A, et al. (2006a). A phosphatase complex that dephosphorylates gammaH2AX regulates DNA damage checkpoint recovery. Nature 439, 497–501. [PubMed: 16299494]

Keogh MC, Mennella TA, Sawa C, Berthelet S, Krogan NJ, Wolek A, Podolny V, Carpenter LR, Greenblatt JF, Baetz K, et al. (2006b). The Saccharomyces cerevisiae histone H2A variant Htz1 is acetylated by NuA4. Genes Dev 20, 660–665. [PubMed: 16543219]

Kerr SC, Azzouz N, Fuchs SM, Collart MA, Strahl BD, Corbett AH, and Laribee RN (2011). The Ccr4-Not complex interacts with the mRNA export machinery. PLoS One 6, e18302. [PubMed: 21464899]

Kiely CM, Marguerat S, Garcia JF, Madhani HD, Bahler J, and Winston F (2011). Spt6 is required for heterochromatic silencing in the fission yeast Schizosaccharomyces pombe. Mol Cell Biol 31, 4193–4204. [PubMed: 21844224]

Kruk JA, Dutta A, Fu J, Gilmour DS, and Reese JC (2011). The multifunctional Ccr4-Not complex directly promotes transcription elongation. Genes Dev 25, 581–593. [PubMed: 21406554]

Kwak H, and Lis JT (2013). Control of transcriptional elongation. Annu Rev Genet 47, 483–508. [PubMed: 24050178]

Livak KJ, Wills QF, Tipping AJ, Datta K, Mittal R, Goldson AJ, Sexton DW, and Holmes CC (2013). Methods for qPCR gene expression profiling applied to 1440 lymphoblastoid single cells. Methods 59, 71–79. [PubMed: 23079396]

Maillet L, Tu C, Hong YK, Shuster EO, and Collart MA (2000). The essential function of Not1 lies within the Ccr4-Not complex. J Mol Biol 303, 131–143. [PubMed: 11023781]

Manukyan A, Zhang J, Thippeswamy U, Yang J, Zavala N, Mudannayake MP, Asmussen M, Schneider C, and Schneider BL (2008). Ccr4 alters cell size in yeast by modulating the timing of CLN1 and CLN2 expression. Genetics 179, 345–357. [PubMed: 18493058]

Mayer A, Heidemann M, Lidschreiber M, Schreieck A, Sun M, Hintermair C, Kremmer E, Eick D, and Cramer P (2012). CTD tyrosine phosphorylation impairs termination factor recruitment to RNA polymerase II. Science 336, 1723–1725. [PubMed: 22745433]

Mayer A, Lidschreiber M, Siebert M, Leike K, Soding J, and Cramer P (2010). Uniform transitions of the general RNA polymerase II transcription complex. Nat Struct Mol Biol 17, 1272–1278. [PubMed: 20818391]

McCullough L, Connell Z, Petersen C, and Formosa T (2015). The Abundant Histone Chaperones Spt6 and FACT Collaborate to Assemble, Inspect, and Maintain Chromatin Structure in Saccharomyces cerevisiae. Genetics 201, 1031–1045. [PubMed: 26416482]

McDonald SM, Close D, Xin H, Formosa T, and Hill CP (2010). Structure and biological importance of the Spn1-Spt6 interaction, and its regulatory role in nucleosome binding. Mol Cell 40, 725–735. [PubMed: 21094070]

Medina DA, Jordan-Pla A, Millan-Zambrano G, Chavez S, Choder M, and Perez-Ortin JE (2014). Cytoplasmic 5'−3' exonuclease Xrn1p is also a genome-wide transcription factor in yeast. Front Genet 5, 1. [PubMed: 24567736]

Miller JE, and Reese JC (2012). Ccr4-Not complex: the control freak of eukaryotic cells. Crit Rev Biochem Mol Biol 47, 315–333. [PubMed: 22416820]

Moqtaderi Z, Yale JD, Struhl K, and Buratowski S (1996). Yeast homologues of higher eukaryotic TFIID subunits. Proc Natl Acad Sci U S A 93, 14654–14658. [PubMed: 8962109]

Muhlrad D, Decker CJ, and Parker R (1994). Deadenylation of the unstable mRNA encoded by the yeast MFA2 gene leads to decapping followed by 5'-->3' digestion of the transcript. Genes Dev 8, 855–866. [PubMed: 7926773]

Nasmyth K (1993). Control of the yeast cell cycle by the Cdc28 protein kinase. Curr Opin Cell Biol 5, 166–179. [PubMed: 8507488]

Neigeborn L, Celenza JL, and Carlson M (1987). SSN20 is an essential gene with mutant alleles that suppress defects in SUC2 transcription in Saccharomyces cerevisiae. Mol Cell Biol 7, 672–678. [PubMed: 3547080]

Oesterreich FC, Herzel L, Straube K, Hujer K, Howard J, and Neugebauer KM (2016). Splicing of Nascent RNA Coincides with Intron Exit from RNA Polymerase II. Cell 165, 372–381. [PubMed: 27020755]

Passos DO, and Parker R (2008). Analysis of cytoplasmic mRNA decay in Saccharomyces cerevisiae. Methods Enzymol 448, 409–427. [PubMed: 19111187]

Perales R, Erickson B, Zhang L, Kim H, Valiquett E, and Bentley D (2013). Gene promoters dictate histone occupancy within genes. EMBO J 32, 2645–2656. [PubMed: 24013117]

Reese JC (2013). The control of elongation by the yeast Ccr4-not complex. Biochim Biophys Acta 1829, 127–133. [PubMed: 22975735]

Rudner AD, Hardwick KG, and Murray AW (2000). Cdc28 activates exit from mitosis in budding yeast. J Cell Biol 149, 1361–1376. [PubMed: 10871278]

Schep AN, Buenrostro JD, Denny SK, Schwartz K, Sherlock G, and Greenleaf WJ (2015). Structured nucleosome fingerprints enable high-resolution mapping of chromatin architecture within regulatory regions. Genome Res 25, 1757–1770. [PubMed: 26314830]

Schep AN, Wu B, Buenrostro JD, and Greenleaf WJ (2017). chromVAR: inferring transcription-factor-associated accessibility from single-cell epigenomic data. Nat Methods 14, 975–978. [PubMed: 28825706]

Schwabish MA, and Struhl K (2004). Evidence for eviction and rapid deposition of histones upon transcriptional elongation by RNA polymerase II. Mol Cell Biol 24, 10111–10117. [PubMed: 15542822]

Sdano MA, Fulcher JM, Palani S, Chandrasekharan MB, Parnell TJ, Whitby FG, Formosa T, and Hill CP (2017). A novel SH2 recognition mechanism recruits Spt6 to the doubly phosphorylated RNA polymerase II linker at sites of transcription. Elife 6.

Shalem O, Groisman B, Choder M, Dahan O, and Pilpel Y (2011). Transcriptome kinetics is governed by a genome-wide coupling of mRNA production and degradation: a role for RNA Pol II. PLoS Genet 7, e1002273. [PubMed: 21931566]

Shetty A, Kallgren SP, Demel C, Maier KC, Spatt D, Alver BH, Cramer P, Park PJ, and Winston F (2017). Spt5 Plays Vital Roles in the Control of Sense and Antisense Transcription Elongation. Mol Cell 66, 77–88 e75. [PubMed: 28366642]

Siwaszek A, Ukleja M, and Dziembowski A (2014). Proteins involved in the degradation of cytoplasmic mRNA in the major eukaryotic model systems. RNA Biol 11, 1122–1136. [PubMed: 25483043]

Spellman PT, Sherlock G, Zhang MQ, Iyer VR, Anders K, Eisen MB, Brown PO, Botstein D, and Futcher B (1998). Comprehensive identification of cell cycle-regulated genes of the yeast Saccharomyces cerevisiae by microarray hybridization. Mol Biol Cell 9, 3273–3297. [PubMed: 9843569]

Sun M, Lariviere L, Dengl S, Mayer A, and Cramer P (2010). A tandem SH2 domain in transcription elongation factor Spt6 binds the phosphorylated RNA polymerase II C-terminal repeat domain (CTD). J Biol Chem 285, 41597–41603. [PubMed: 20926372]

Sun M, Schwalb B, Pirkl N, Maier KC, Schenk A, Failmezger H, Tresch A, and Cramer P (2013). Global analysis of eukaryotic mRNA degradation reveals Xrn1-dependent buffering of transcript levels. Mol Cell 52, 52–62. [PubMed: 24119399]

Sun M, Schwalb B, Schulz D, Pirkl N, Etzold S, Lariviere L, Maier KC, Seizl M, Tresch A, and Cramer P (2012). Comparative dynamic transcriptome analysis (cDTA) reveals mutual feedback between mRNA synthesis and degradation. Genome Res 22, 1350–1359. [PubMed: 22466169]

Swanson MS, Carlson M, and Winston F (1990). SPT6, an essential gene that affects transcription in Saccharomyces cerevisiae, encodes a nuclear protein with an extremely acidic amino terminus. Mol Cell Biol 10, 4935–4941. [PubMed: 2201908]

Traven A, Beilharz TH, Lo TL, Lueder F, Preiss T, and Heierhorst J (2009). The Ccr4-Pop2-NOT mRNA deadenylase contributes to septin organization in Saccharomyces cerevisiae. Genetics 182, 955–966. [PubMed: 19487562]

Trcek T, Larson DR, Moldon A, Query CC, and Singer RH (2011). Single-molecule mRNA decay measurements reveal promoter- regulated mRNA stability in yeast. Cell 147, 1484–1497. [PubMed: 22196726]

Tucker M, Staples RR, Valencia-Sanchez MA, Muhlrad D, and Parker R (2002). Ccr4p is the catalytic subunit of a Ccr4p/Pop2p/Notp mRNA deadenylase complex in Saccharomyces cerevisiae. EMBO J 21, 1427–1436. [PubMed: 11889048]

Tucker M, Valencia-Sanchez MA, Staples RR, Chen J, Denis CL, and Parker R (2001). The transcription factor associated Ccr4 and Caf1 proteins are components of the major cytoplasmic mRNA deadenylase in Saccharomyces cerevisiae. Cell 104, 377–386. [PubMed: 11239395]

Villanyi Z, and Collart MA (2015). Ccr4-Not is at the core of the eukaryotic gene expression circuitry. Biochem Soc Trans 43, 1253–1258. [PubMed: 26614669]

Westmoreland TJ, Marks JR, Olson JA, Jr., Thompson EM, Resnick MA, and Bennett CB (2004). Cell cycle progression in G1 and S phases is CCR4 dependent following ionizing radiation or replication stress in Saccharomyces cerevisiae. Eukaryot Cell 3, 430–446. [PubMed: 15075273]

Wilusz CJ, Wormington M, and Peltz SW (2001). The cap-to-tail guide to mRNA turnover. Nat Rev Mol Cell Biol 2, 237–246. [PubMed: 11283721]

Yoh SM, Cho H, Pickle L, Evans RM, and Jones KA (2007). The Spt6 SH2 domain binds Ser2-P RNAPII to direct Iws1-dependent mRNA splicing and export. Genes Dev 21, 160–174. [PubMed: 17234882]

Zhang L, Fletcher AG, Cheung V, Winston F, and Stargell LA (2008). Spn1 regulates the recruitment of Spt6 and the Swi/Snf complex during transcriptional activation by RNA polymerase II. Mol Cell Biol 28, 1393–1403. [PubMed: 18086892]

Zobeck KL, Buckley MS, Zipfel WR, and Lis JT (2010). Recruitment timing and dynamics of transcription factors at the Hsp70 loci in living cells. Mol Cell 40, 965–975. [PubMed: 21172661]

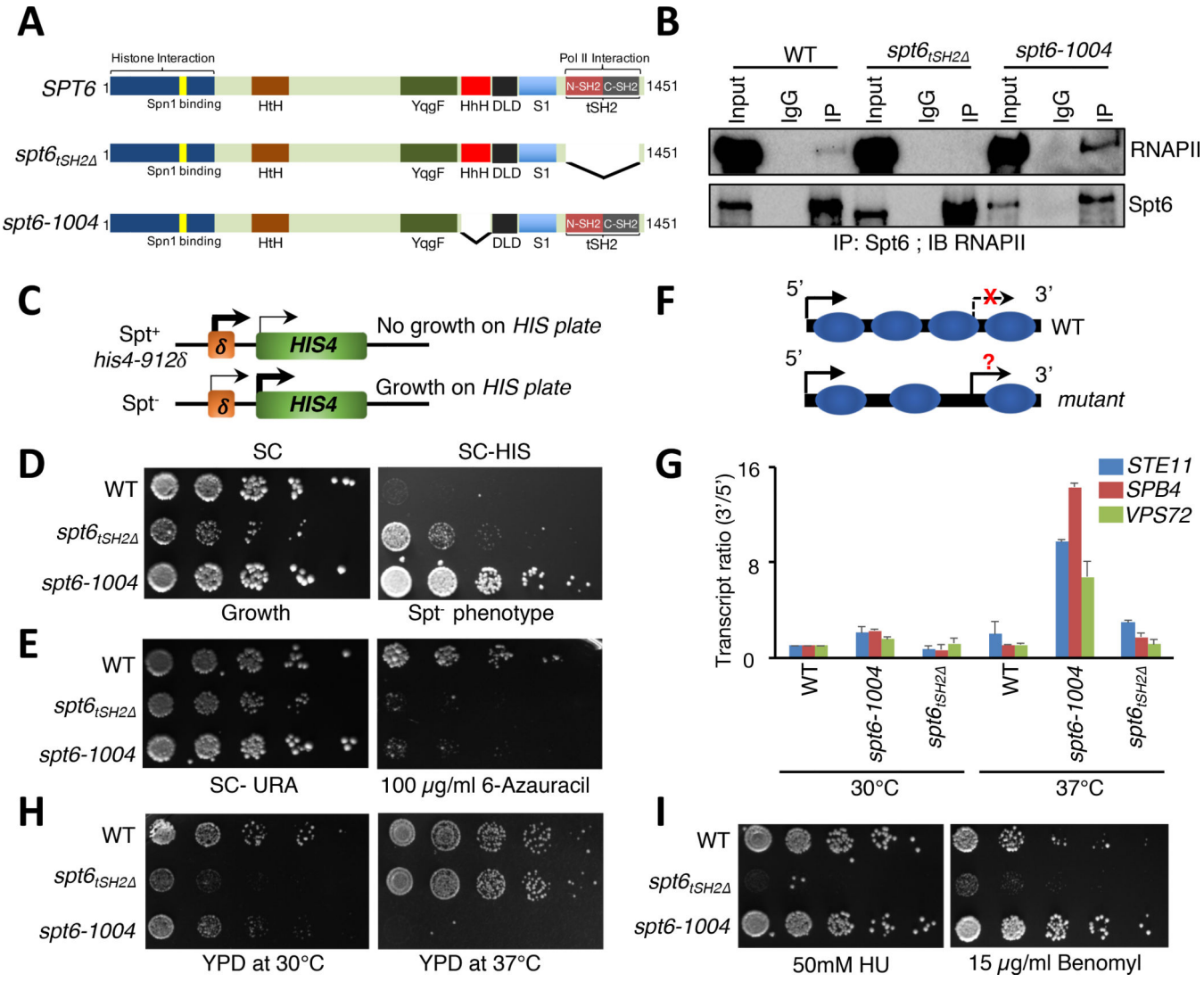

Figure 1. Uncoupling Spt6-RNAPII interaction reveals distinct Spt6 phenotypes

(A) Domain organization and forms of Spt6 used in this study. HtH (Helix-turn-Helix domain); YqgF (RNase H-like domain); HhH (Helix-hairpin-Helix domain); S1 (S1 domain); DLD (Death-like-Domain); and tSH2 (Tandem Src2 homology domain). (B) Spt6 interacts with RNAPII via a tSH2 domain. Co-immunoprecipitation experiments were performed for Spt6 and RNAPII, and interaction was assessed by immunoblot analysis with various phospho-Ser2-CTD specific antibodies. (C) Schematic of the Spt- phenotype. Insertion of a Ty element at the *HIS4* locus suppresses expression. Spt- mutants allow expression of *HIS4* and growth on medium lacking histidine. (D) Spt- phenotypic assay. 5-fold serial dilutions of the indicated strains were spotted on synthetic complete (SC) and SC medium lacking histidine. (E) Spt6 is required for transcription elongation. Spotting assays showing the sensitivity of *spt6* mutants on 6-azauracil plates. (F) Schematic illustrating normal and cryptic (intragenic) transcription. In wild-type (WT) cells, intragenic sites of transcription are normally suppressed but can be activated in mutants that perturb chromatin integrity. (G) qRT-PCR assay to validate the generation of intragenic sense transcripts using

primers spanning the 5’ and the 3’ regions of *STE11, SPB4,* and *VPS72* genes in WT, *spt6–1004,* and $spt6_{tSH2\Delta}$ mutant cells. (H) and (I) Spotting assays showing functionally distinct phenotypes of the *spt6–1004* and $spt6_{tSH2\Delta}$ mutants upon exposure to heat and genotoxic agents, respectively. 5-fold serial dilutions were spotted on the indicated medium. Plates were incubated at 30°C or 37°C and photographs were taken after 4 days.

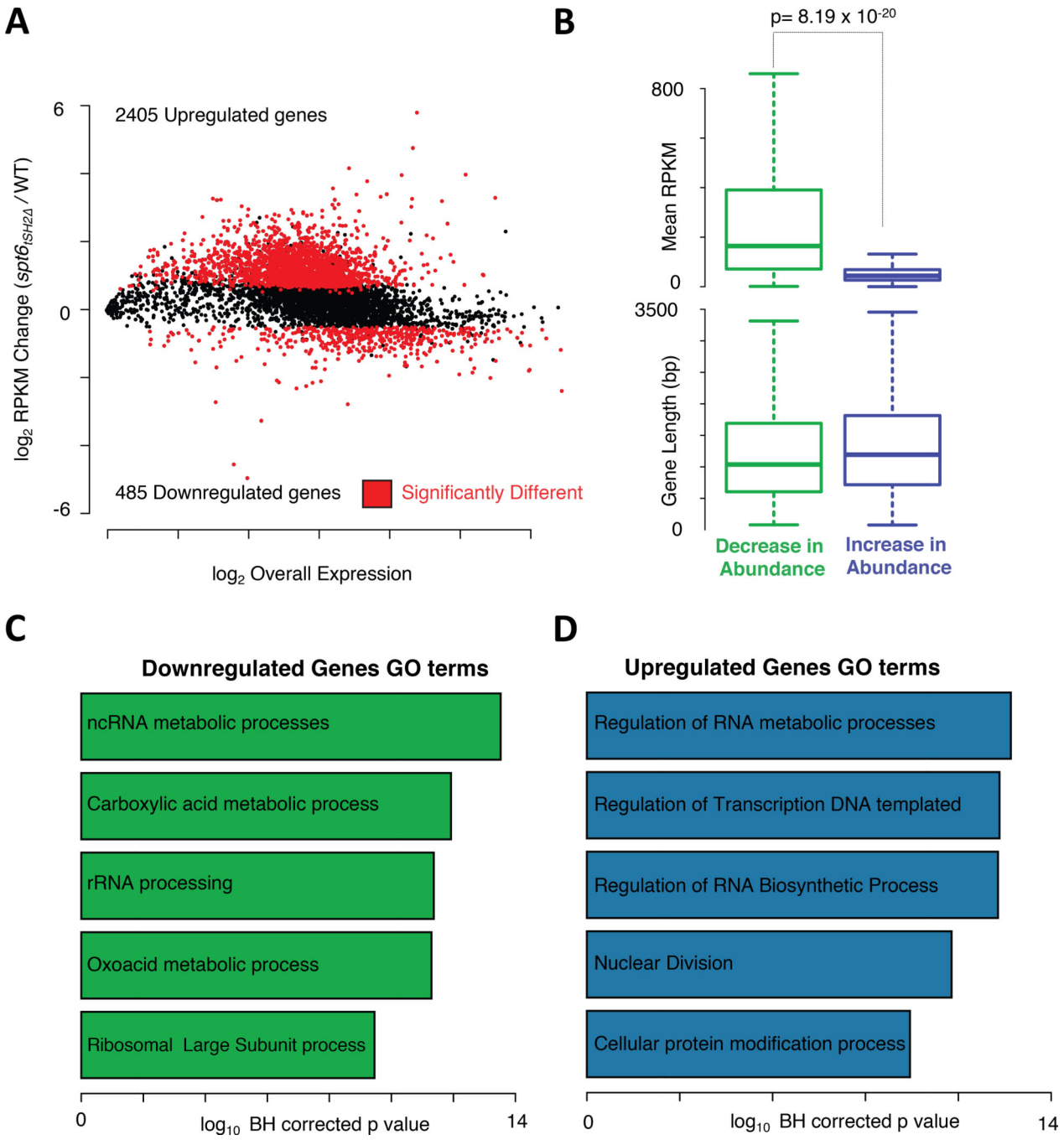

Figure 2. Spt6-RNAPII Interaction Regulates Global Transcriptome.

(A) MA plot showing changes in the gene expression patterns in the *spt6*$_{tSH2\Delta}$ mutant normalized to the WT transcriptome. (B) Box plots showing the correlation between the up/downregulated genes and expression levels and gene length. (C) and (D) Gene Ontology (GO) analysis of the downregulated and upregulated genes, respectively, in the *spt6*$_{tSH2\Delta}$ mutant.

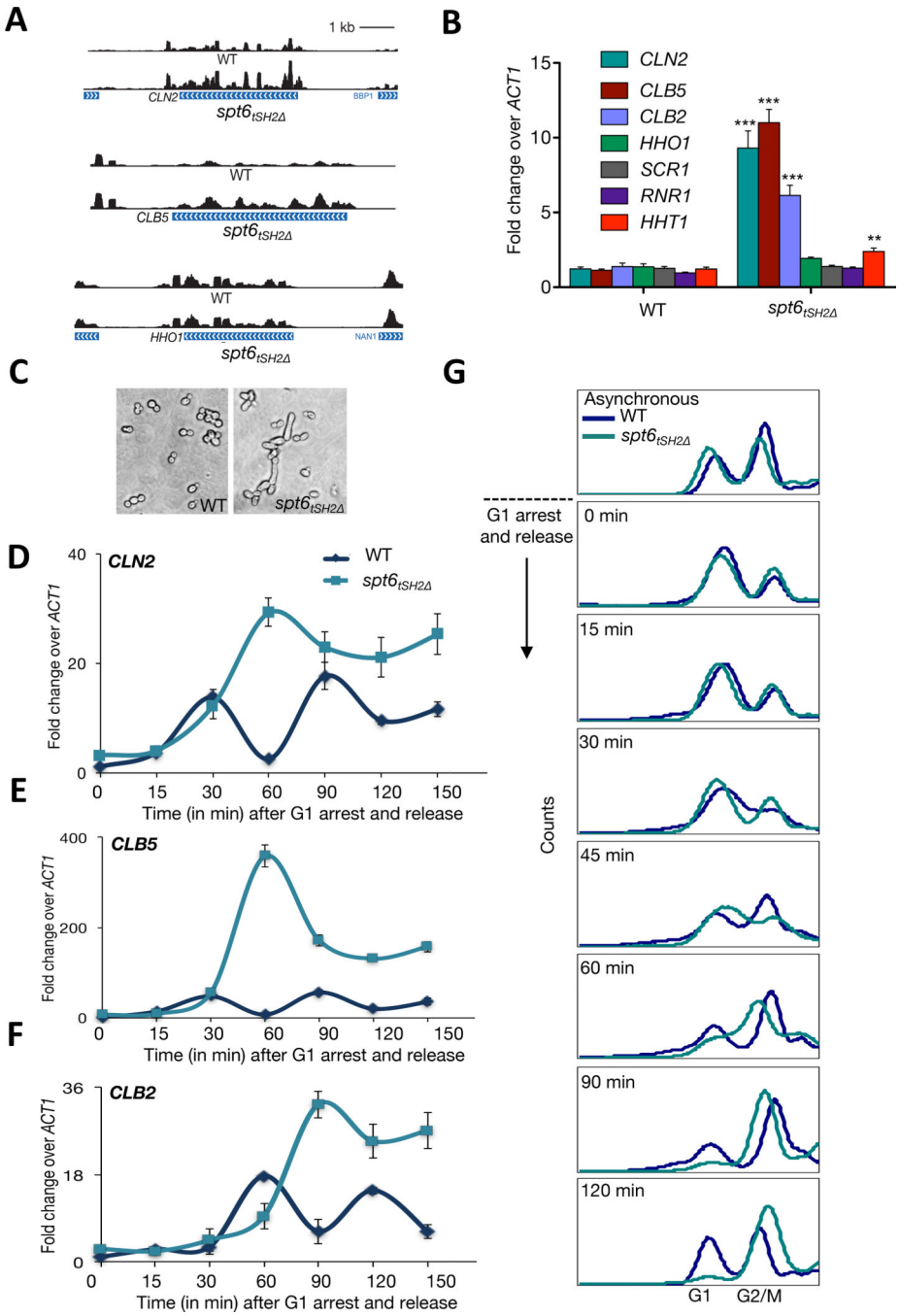

Figure 3. Spt6-RNAPII Interaction is required for cell cycle progression.

(A) Representative tracks of *CLN2, CLB5,* and *HHO1* transcripts in the WT and $spt6_{tSH2\Delta}$ mutant. (B) qRT-PCR analysis of the representative transcripts in the WT and $spt6_{tSH2\Delta}$ mutant. Shown are the mean ± SD for three biological replicates. The p values were calculated using Student's t test. ** represents a p value less than 0.01. (C) DIC image showing the morphology of the WT and $spt6_{tSH2\Delta}$ mutant cells. (D-F) qRT-PCR quantitation of *CLN2, CLB5,* and *CLB2* transcripts in WT and $spt6_{tSH2\Delta}$ mutant cells arrested in G1 and released into fresh medium. Shown are the mean and SD for three biological replicates. (G)

WT and *spt6*$_{tSH2\Delta}$ mutant cells were arrested in G1 using α-factor and released into fresh medium; samples at different time points were analyzed by flow cytometry for DNA content.

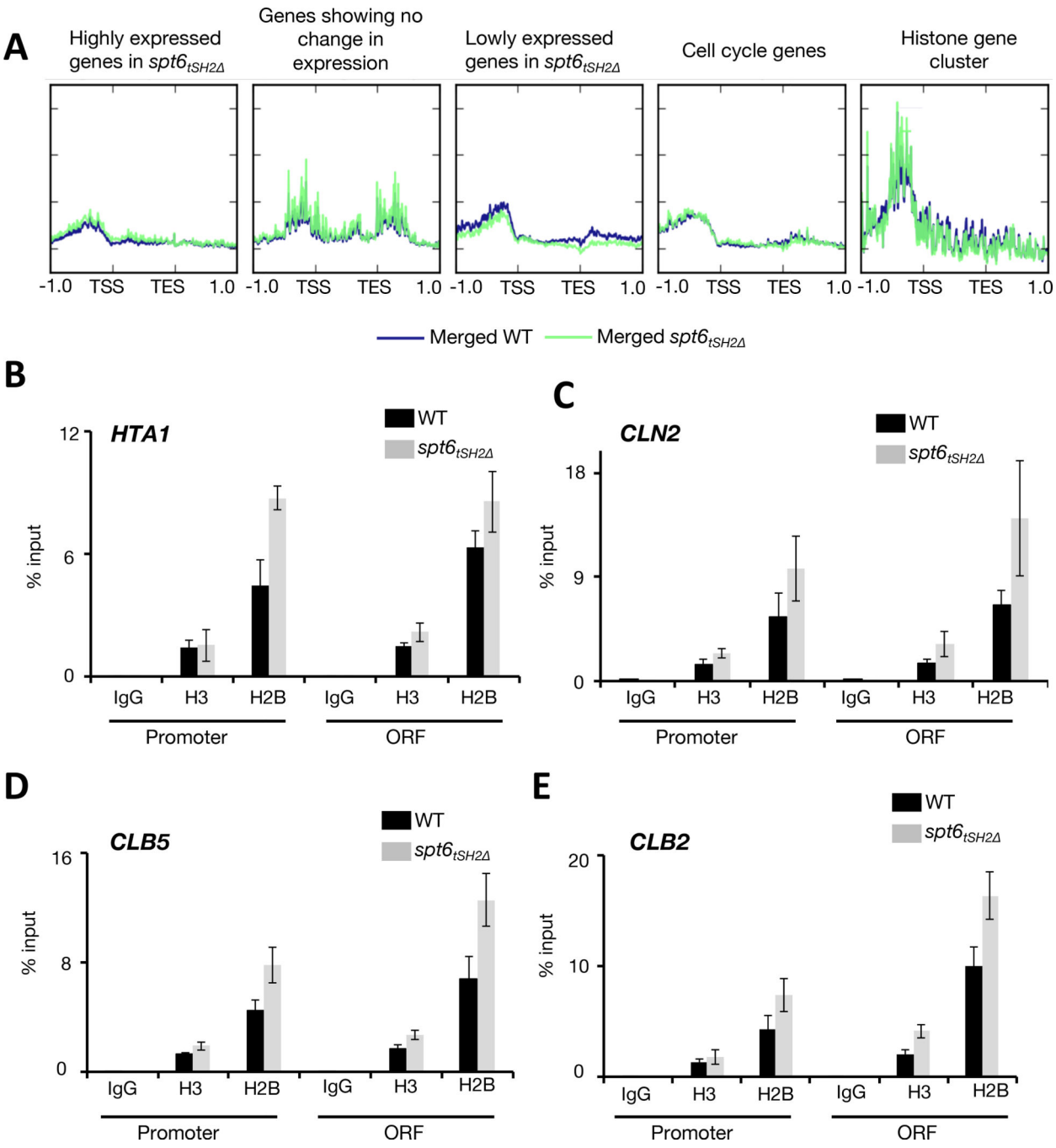

Figure 4. Spt6-RNAPII interaction is not required to maintain promoter fidelity.

(A) Metagene analysis of the ATAC-seq signals showing tracks for the changes in nucleosome occupancy in WT and the *spt6*$_{tSH2\Delta}$ mutant under different conditions. The blue tracks represent the WT and the green tracks represent the *spt6*$_{tSH2\Delta}$ mutant. Labels above each panel indicate the classification of genes based on their expression changes (B-E) ChIP-qPCR to detect the occupancy of histone H3 and H2B at the promoters and open reading frames (ORFs) of *HTA1*, *CLN2*, *CLB5,* and *CLB2,* respectively. Data are

represented as mean ± SD of the percent input method of enrichments in three independent biological replicate experiments.

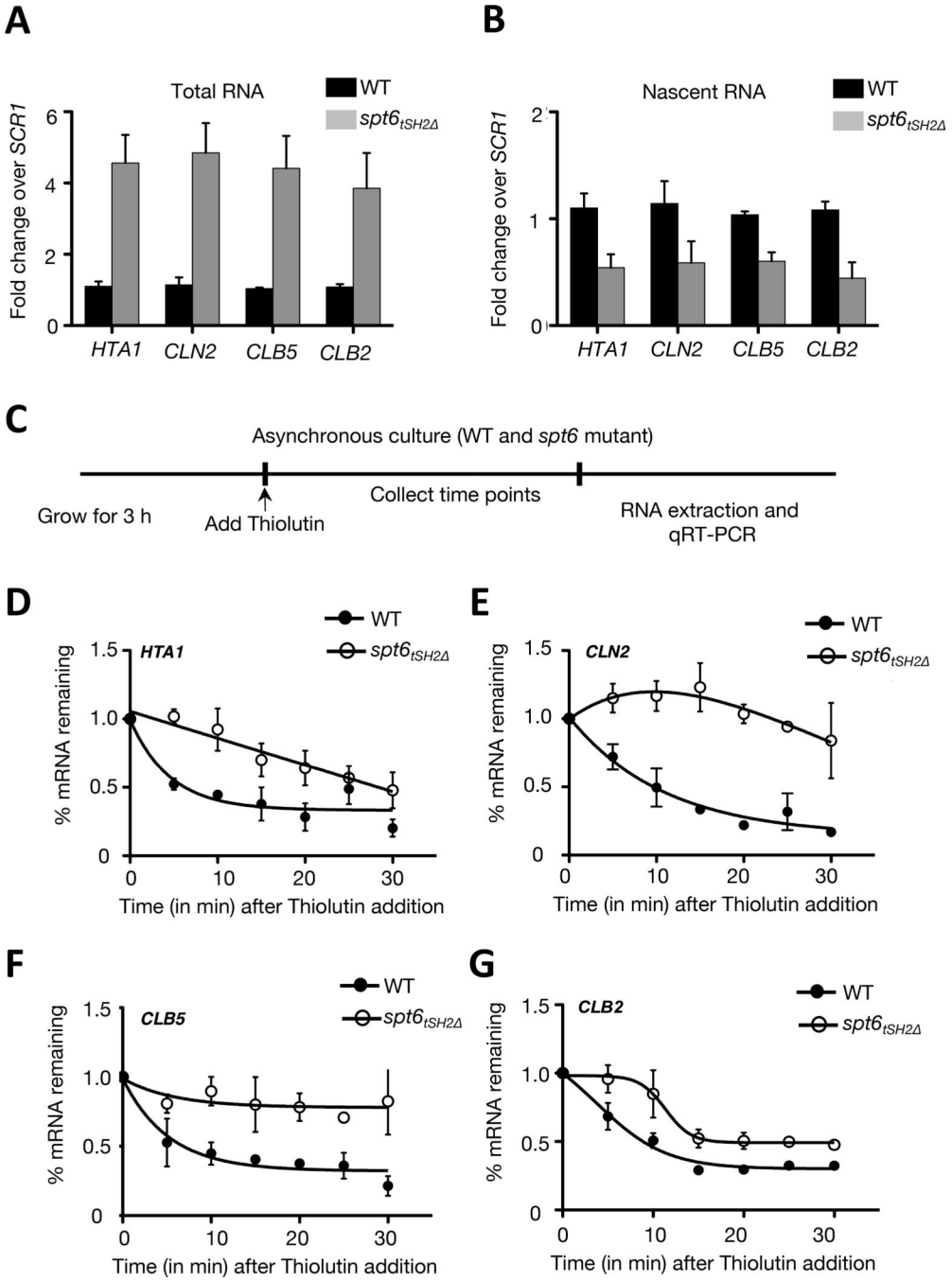

Figure 5. Spt6 is essential for regulation of mRNA turnover.

Spt6 is required for mRNA turnover. (A) qRT-PCR analysis of *HTA1, CLN2, CLB5, and CLB2* from total RNA extracted from WT and $spt6_{tSH2\Delta}$ mutant cells (B) The same transcripts analyzed from RNA extracted from the chromatin fraction (nascent chromatin) (C) Schematic representation of the experiment for the treatment of WT and $spt6_{tSH2\Delta}$ mutant cells with Thiolutin to assess mRNA stability. (D-G) are the qRT-PCR results showing changes in *HTA1, CLN2, CLB5,* and *CLB2* transcripts, respectively, at the

indicated timepoints after Thiolutin addition. Data are the mean and SD for three biological replicates. The p values were calculated using Student's t test.

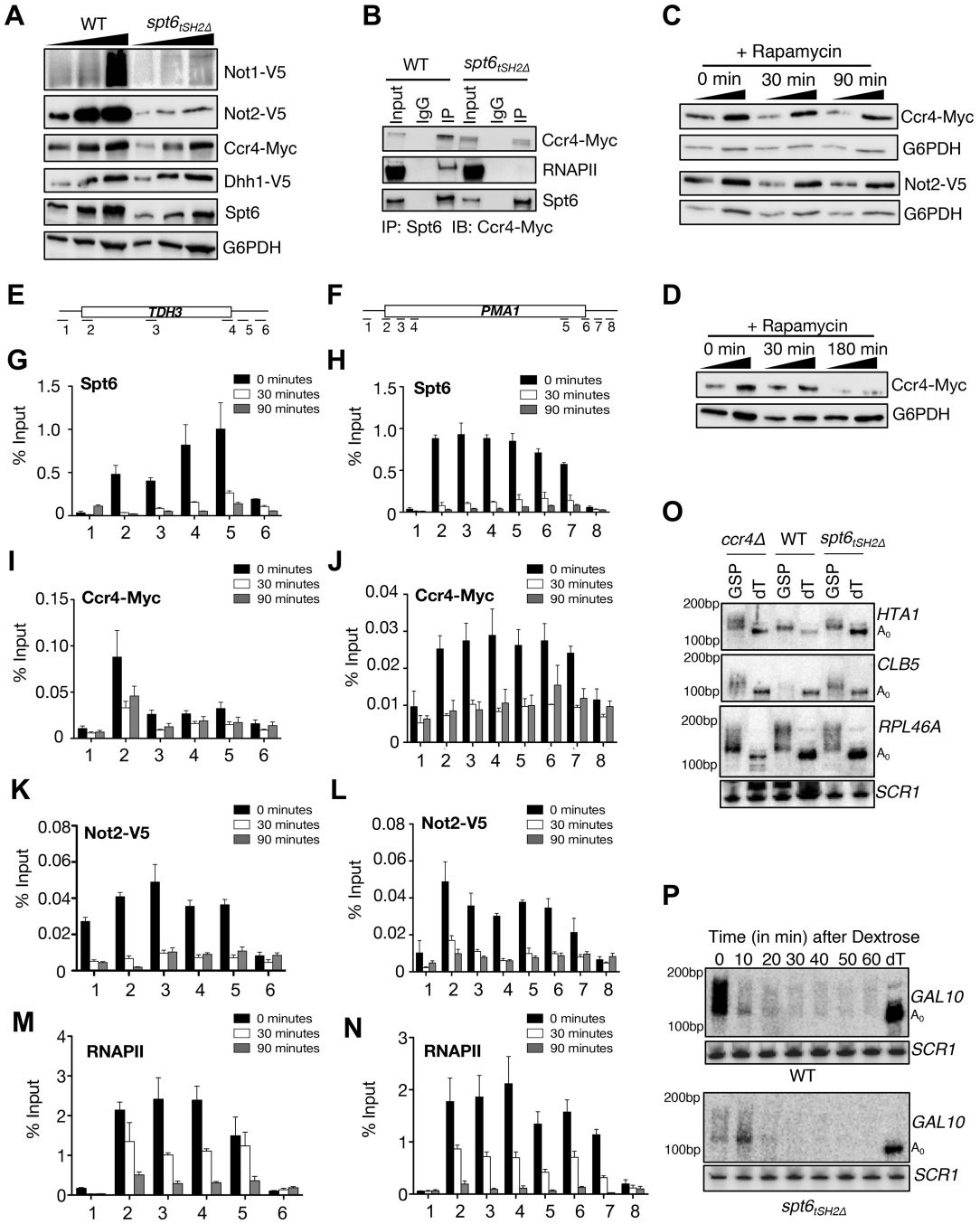

Figure 6. Spt6 recruits the Ccr4-Not complex to chromatin.

Interaction of Spt6 with RNAPII is required for optimal levels of Ccr4-Not complex members. (A) Exponentially growing WT and *spt6*$_{tSH2\Delta}$ mutant cells were subjected to immunoblot analysis (after TCA lysis) to detect changes in the levels of Ccr4-Not complex members (B) Co-immunoprecipitation showing an interaction between Spt6 and Ccr4 in WT and the *spt6*$_{tSH2\Delta}$ mutant. (C) and (D) Immunoblots showing changes in the levels of Ccr4 and Not2 with Spt6 anchor-away at 30, 90 minutes and 3h, respectively. (E) and (F) Schematic representation of the primer locations across *PMA1* and *TDH3* genes. (G) and

(H) ChIP-qPCR of Spt6 kinetics on *PMA1* and *TDH3* genes following rapamycin treatment. ChIP-qPCR showing changes in the occupancy of Ccr4 (I and J) and Not2 (K and L) and RNAPII (M and N) on *PMA1* and *TDH3* genes respectively, following Spt6 depletion. While Spt6 and Ccr4/Not2 are no longer detectable at the 30 minute time-point, we note that RNAPII is still detected, thereby suggesting a role for Spt6 in recruitment of Ccr4-Not (O) Spt6 is required for proper mRNA metabolism and poly(A) tail length. Total RNA was isolated using acid phenol method and 10μg was digested with RNAse H in the presence of gene specific primer (GSP) and/or oligo-$dT_{12–16}$ (dT); A_0 represents the completely deadenylated RNA species. Use of the GSP alone gives the length of the poly(A) tail whereas use of the GSP with dT allows for the determination of A_0. Total RNA was separated in urea-PAGE, blotted on to membranes and probed with oligo probes. (P) High resolution PAGE Northern blot showing the rate of deadenylation of *GAL10* mRNA.

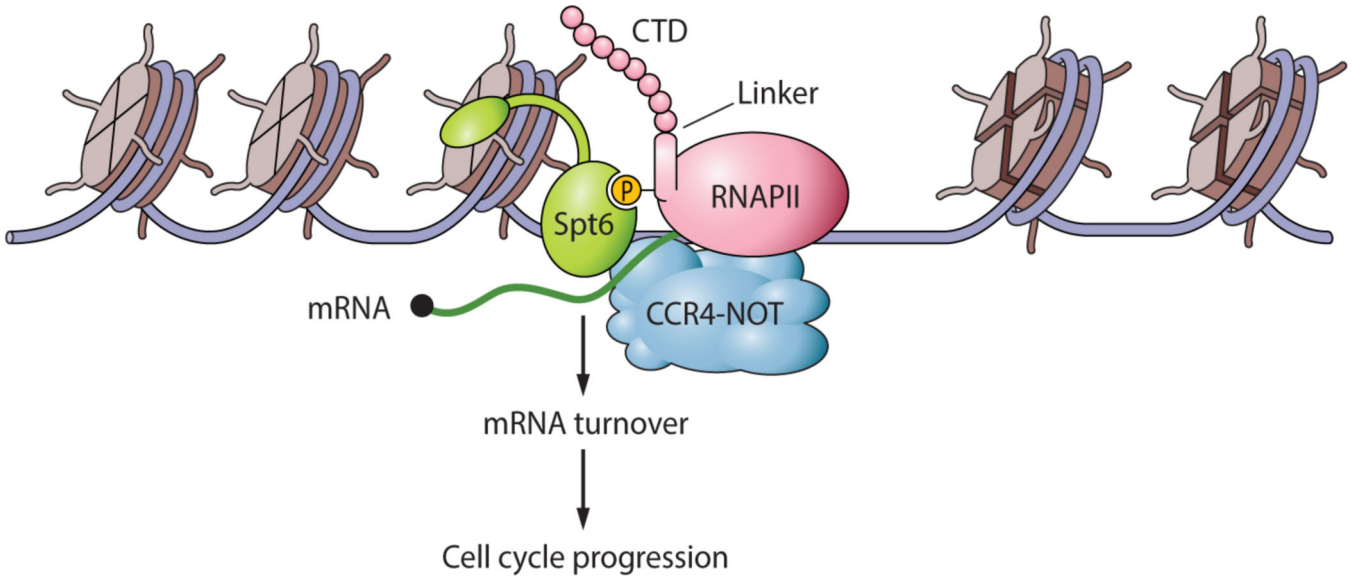

Figure 7. Model showing the connections between Spt6 and the regulation of mRNA turnover.

The model summarizes our finding that Spt6-RNAPII association is key to the recruitment and activity of the Ccr4-Not complex that regulates mRNA turnover. Uncoupling of Spt6 and RNAPII produces increased amounts of cell cycle-associated mRNAs (due to lack of turnover of a broad range of mRNAs) that cause cell cycle defects. Our model depicts Spt6 associating with a newly described phosphorylated linker region in RNAPII that has been found to bind Spt6; however, the Spt6 chaperone also interacts with phosphorylated residues in the RNAPII C-terminal domain (CTD) (not shown; see text for details). These results uncover a previously unknown function for the Spt6 histone chaperone in transcriptional regulation.

KEY RESOURCES TABLE

REAGENT or RESOURCE	SOURCE	IDENTIFIER
Antibodies		
Anti-V5 antibody. Polyclonal	Bethyl labs	Catalog #A190–220A
Anti-Myc antibody, Monoclonal	EMD Millipore	Catalog # 050419
Anti RNAPII Ser2 monoclonal, (Clone 9E10)	Active Motif	Catalog # 61084
Anti-Spt6, polyclonal	In House	
Anti-histone H3 antibody, polyclonal	In House	
Anti-histone H2B antibody, polyclonal	Active Motif	Catalog # 39328
Normal rabbit serum	Cell Signaling Technology	Catalog # 2729S
Anti-G6PDH antibody, polyclonal	Sigma	Catalog # A9521–1VL
ChIP grade RNAPII antibody	BioLegend	Catalog # 664912
HRP-conjugated anti-rabbit	GE Healthcare	Catalog # NA934V
HRP-conjugated anti-mouse	GE Healthcare	Catalog # NA931V
Chemicals, Peptides, and Recombinant Proteins		
6-Azauracil	SIGMA (Roche)	Catalog # A1757
Benomyl	SIGMA (Roche)	Catalog # 45339
Hydroxyurea	SIGMA (Roche)	Catalog # H8627
RNAseH	Promega	Catalog # M4281
T4 Polynucleotide Kinase	NEB	Catalog # M0201S
ULTRAhyb Oligo Buffer	Thermo Fisher Scientific	Catalog # AM8663
SSIII RT reverse transcriptase	Thermo Fisher Scientific	Catalog # 18080–044
Acid phenol Chloroform	Ambion/Thermo Fisher Scientific	Catalog # AM9722
Zeta Probe Blotting membrane	Biorad	Catalog # 1620153
Rapamycin	SIGMA (Roche)	Catalog # R8781
cOMPLETE, EDTA free protease inhibitor tablets	SIGMA (Roche)	Catalog # 11873580001
PhosSTOP phosphatase inhibitor tablets	SIGMA (Roche)	Catalog # 04906845001
Century TM Plus RNA markers	Thermo Fisher Scientific	Catalog # AM7145
Gel Loading Buffer II	Thermo Fisher Scientific	Catalog # AM8547
iTaq™ Universal SYBR ® Green Supermix	Biorad	Catalog # 172–5124
Protein A Agarose	SIGMA (Roche)	Catalog # 11134515001
Propidium Iodide	Thermo Fisher Scientific	Catalog # P3566
Thiolutin	Abcam	Catalog # ab143556
Dynabeads Protein G	Thermo Fisher Scientific	Catalog # 10009D
SPRI Beads (Agencourt AMPure XP)	Beckman Coulter	Catalog # A63881
α-Factor Mating pheromone	Genscript	Catalog # 59804–28–4
Critical Commercial Assays		
TruSeq Stranded Total RNA with RiboZero Gold Library Prep Kit.	Illumina	Catalog # RS-122–2301
Deposited Data		

REAGENT or RESOURCE	SOURCE	IDENTIFIER
RNAseq and ATAC seq data	This study	GEO:GSE111815
Raw data for Northern Blots and Immunoblots	This Study	Mendeley:http://dx.doi.org/10.17632/tnx4py69j8
Experimental Models: *S.serevisiae* strains		
MATa leu2 trp1-Δ63 ura3 his4–912∂ lys2–128∂	Winston Lab	FY2181
MATa leu2 trp1-Δ63 ura3 his4–912∂ lys2–128∂ spt6–1004	Winston Lab	FY2180
MATa leu2 trp1-Δ63 ura3 his4–912∂ lys2–128∂ CCR4–9MYC::kanMX	This study	RDY20171
MATa leu2 trp1-Δ63 ura3 his4–912∂ lys2–128∂ spt6tSH2::natMX	This study	RDY20172
MATa leu2 trp1-Δ63 ura3 his4–912∂ lys2–128∂ spt6tSH2::natMX CCR4–9MYC::kanMX	This study	RDY20173
MATa ade2–1 trp1–1can1–100 leu2–3, 112 his3–11, 15 ura3 tor1–1 frp1::NAT RPL13A-2XFKBP12::TRP1 SPT6-FRB::KanMX	This study	yDZ001
Oligonucleotides		
Oligos	This study and other sources	Supplementary Table 2
Recombinant DNA		
NOT1-V5 (plasmid),	DNASU	Catalog # ScCD00102519
NOT2-V5 (plasmid)	DNASU	Catalog # ScCD00103149
DHH1-V5 (plasmid)	DNASU	Catalog # ScCD00102795